2019

WAAPI

Wild Area Aerial Protective Inspector

Proposal for 2018-2019 Undergraduate Individual Aircraft Linear Infrastructure Inspection UAS

SHARIF UNIVERSITY OF TECHNOLOGY

Signature Sheet

Mina Khalilzade Fathi

AIAA 921462

Prof. S. Mohammad B. Malaek

Faculty Adviser

Unmanned Platforms And Subsystems

Unmanned Aerial System

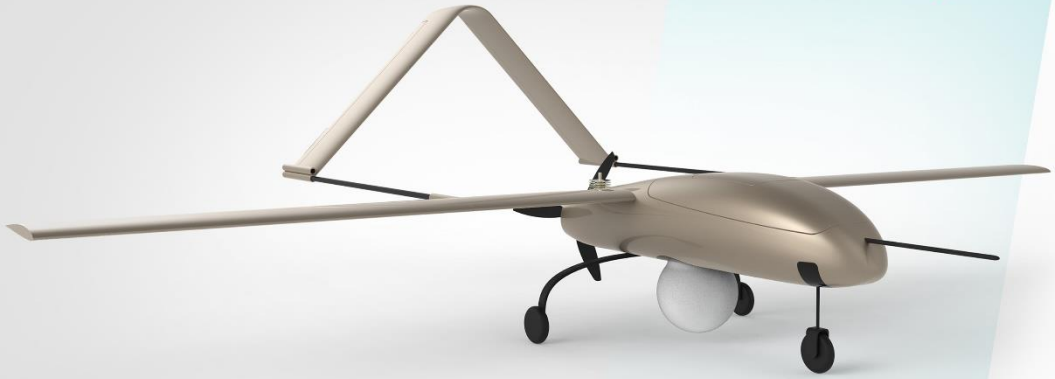

Car-top launcher is a convenient, reliable and low-cost option for runway

Professional radio control and telemetry with an extraordinary range in the radio system in the free ISM band. FHSS configurable frequency hopping with excellent synchronization and fast recovery.

Portable Ground Control Station. includes all the necessary components to perform missions from 100Km up to 200Km. User friendly software interface

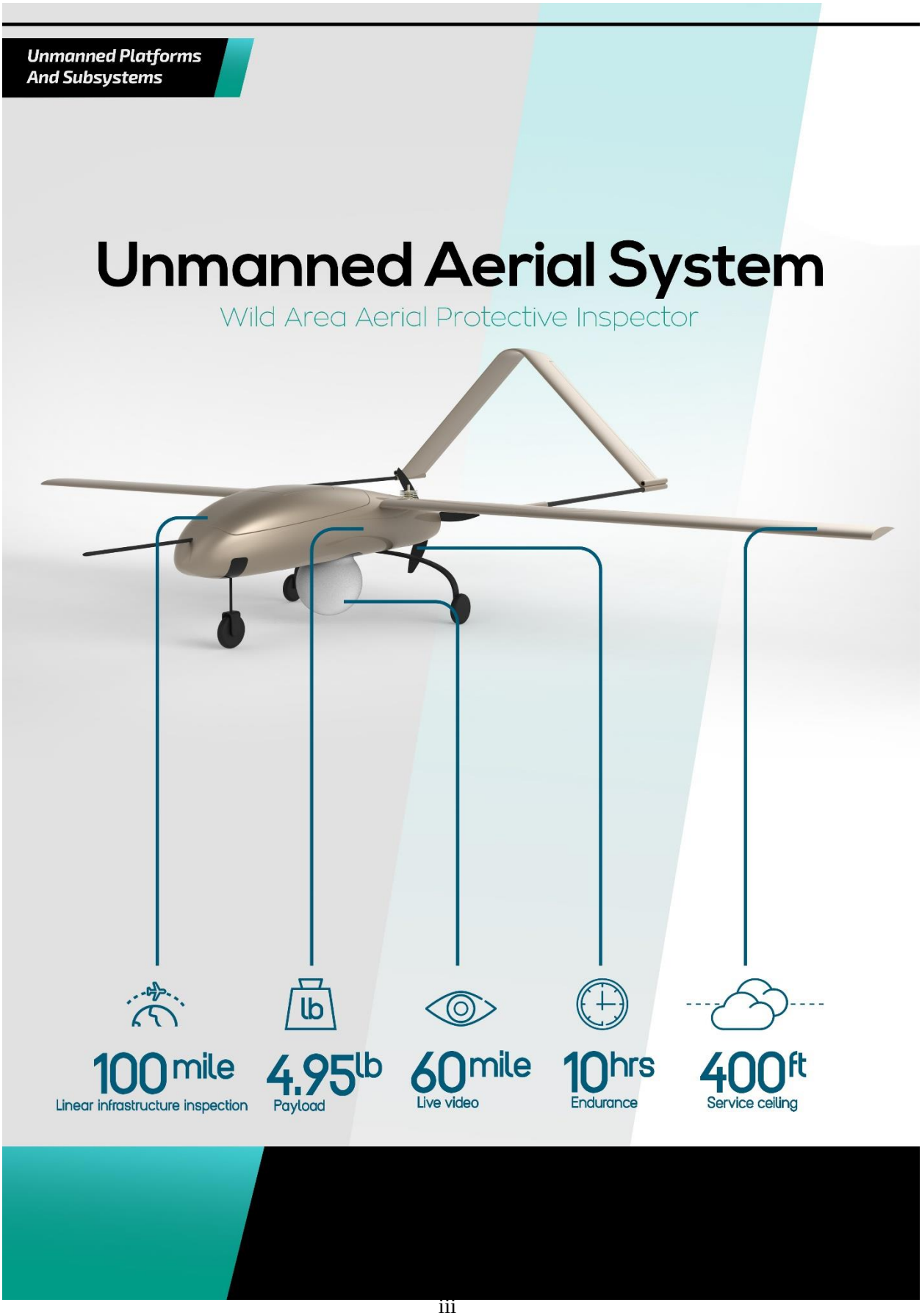
Unmanned Platforms
And Subsystems
Unmanned Aerial System
Wild Area Aerial Protective Inspector
100 mile
Linear infrastructure inspection
4.95 lb
Payload
60 mile
Live video
10 hrs
Endurance
400 ft
Service ceiling

Compliance Checklist

Specifications:

Table 1-1 UAV specification

Parameter	Value
MTOW	36 lb.
Empty weight	28.75 lb.
Max Payload	4.95 lb.
Wing Area	9 ft^2
Wing Span	10.4 ft.
Length	7.73 ft.
Power Planet	3.1HP
Takeoff Method	Conventional takeoff, Car top launch
Landing Method	Conventional landing, Parachute recovery

Performance:

Table 1-2 UAV's performance parameters

Parameter	Value
Endurance	10 hours
Cruise Speed	82 ft./s
Stall Speed	52 ft./s
Max Cruise Speed	82 ft./s
Takeoff Run	150 ft.
Service ceiling	400 ft.

1 Contents

Table of figures

List of Tables

Acknowledgements

I would like to express my great appreciation to **Mohammad Alizadeh** for the Cost estimation and the proposal integration, **Aref Zamani** for his valuable CAD and **Motahare Karimifard** for her support to complete the proposal.

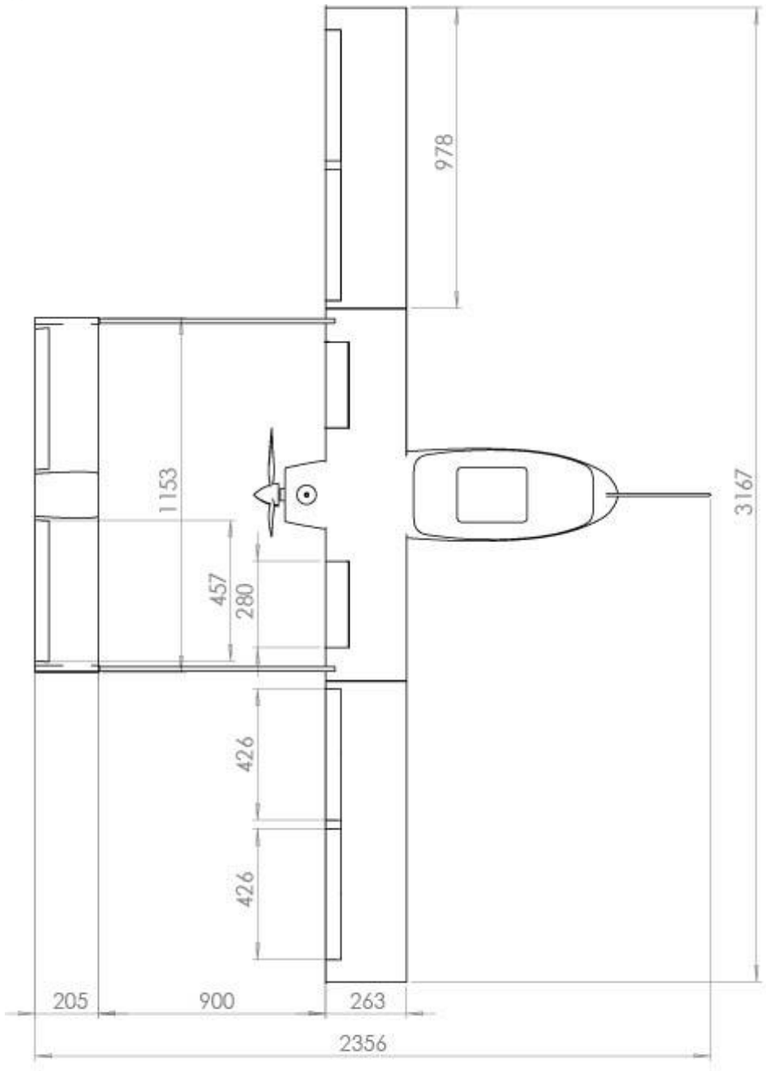

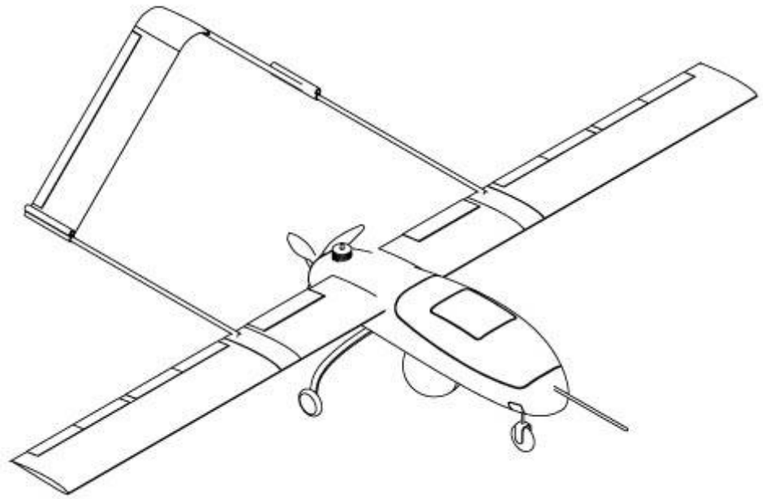

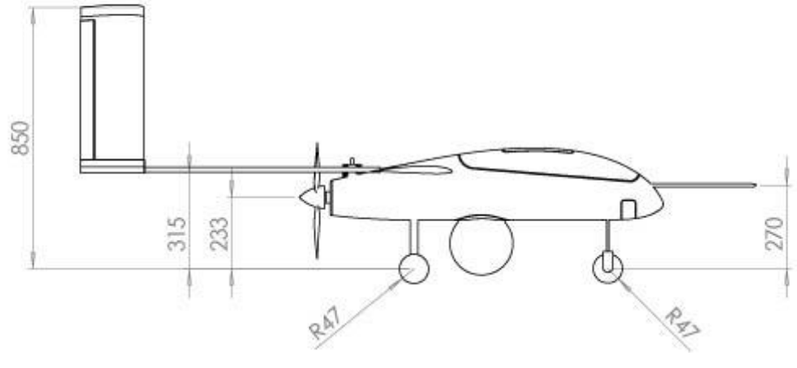

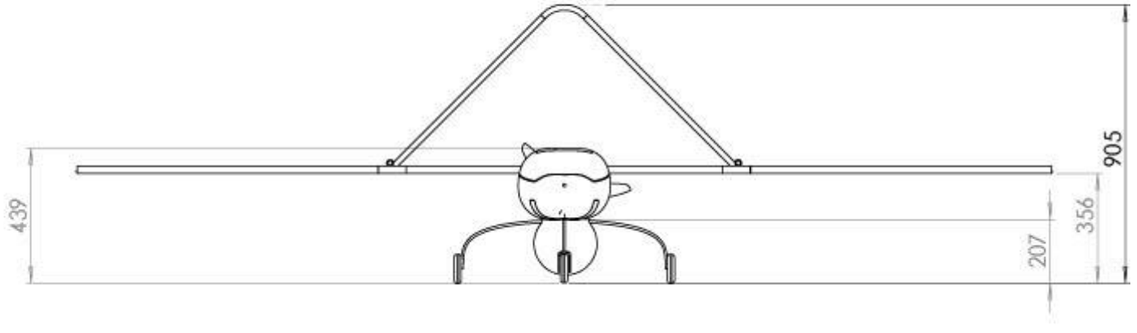

Figure 1–1 3view of WAAPI **All numbers are in mm**

1 Executive Summary

The goal of this proposal was to design an Unmanned Aerial System (UAS). A UAS is much more than the unmanned aircraft. Communications systems, ground control stations, launch and recovery equipment, and support equipment was considered as elements of UAS. The WAAPI was designed to be the most efficient in cost. Major missions set are linear infrastructure inspection for long flight endurance and terrain modeling of larger areas because of this wing type is selected for unmanned aircraft element. By designing the concept of operation for our system as well as applying SHELL theory to the system we Design other elements are designed. If a mission is scheduled outside the FAA Part 107 regulations, WAAPI checks the mission and then lands. Parts of WAPPI is interchangeable to be desired for support. Interchangeable modules that can be replaced over the life of the WAPPI UAV, which causes to remain in operational service indefinitely but have all of the parts replaced. It can carry up to three payloads at the same time. When emergency recovery is occurred or landing on rugged surface, optional payload enters inside the body. Autonomous takeoff and landing and capability of autonomous flight with an autopilot under lost link conditions. Car-top launcher is optional for runway (<500 ft.) As well as can be mounted on car roof and aircraft can be transported when mounted on the car-top launcher with the wing tips removed and secured with safety-pins. WAAPI UAV can be launched from any surface, where a car can reach the takeoff speed, which is approximately 63 fps. The customer have the option of integrating their own payload based on their specific project needs. When landing on the ground as well as in the case of emergency recovery optional payload goes inside the fuselage by an actuator. Ground Data Terminal Up to 60miles analog link for video. WAAPI's portable Ground Control Station includes all the necessary components to perform missions from 100Km up to 200Km.

2 Market Analysis

The small UAV market is anticipated to register a CAGR of over 15% during the forecast period (2019 - 2024). Growing applications of small UAVs in aerial photography, 3D mapping, surveying, and oil and gas pipeline monitoring, among others are propelling the growth of the small UAV market.

Currently, North America holds the major share in the UAV market, globally. This is primarily due to the increasing use of unmanned aerial vehicles, both for commercial and military applications. Asia-Pacific is expected to register the highest CAGR, during the forecast period, due to the growing popularity of UAVs in the Asia-Pacific region, as well as increasing technological developments of drones in the region and changes in regulations. The procurement of UAVs in the region is steadily growing, thereby driving the growth of the UAV market in Asia-Pacific. [1]

Figure 2–1 Small UAV Market - Growth Rate by region (2019-2024)

2.1 North America small UAV market

The North America small UAV market is anticipated to record a CAGR of 9.26% to value USD 897.25 million by 2024. The increasing applications in surveying, aerial photography, 3D mapping, oil and gas pipeline monitoring and similar infrastructure inspection, and real state surveys, are driving the growth of the North American small UAV market.

2.2 Europe Small UAV Market

The Europe Small UAV Market is expected to register a CAGR of more than 8% over the forecast period. South America Small UAV Market. Small UAVs are expected to have a high adoption rate in European countries, with enterprises across different industries investing in these products. However, the regulations relating to the commercial use of small UAVs from CAA and other organizations are more. In countries like the UK, permission from the CAA is required for any commercial work with a drone. Such regulations may pose a challenge to the market growth in the region

2.3 Asia Pacific Small UAV Market

Asia Pacific small UAV market is second largest, only after the North American Market, with China being at the top, followed by India. There has been an increase in demand of UAV in the recent times from both commercial and military sectors.

2.4 South America Small UAV Market

The South America Small UAV market is a growing one and the demand is more for non-military uses. Ranging from border control to anti-piracy operations to fighting organized crime and drug cartels, various countries in the region use the Small UAV for varied reasons. One of the main uses of the Small UAV has been gathering intelligence, doing surveillance and reconnaissance missions in fighting drug cartels and against guerrillas. It is being used for guarding natural resources and stopping human trafficking also. In the few years, Brazil is estimated to be the biggest market.

Our objective is to perform the mission on a recurring basis at the lowest life cycle cost and to the operators for different missions. According to the Overall UAV Market Growth and RFP understanding and consideration of objective, it's decided that designed UAV to do the following missions:

- Linear infrastructure monitoring and inspection, including electrical power transmission, pipelines, roads, and railways.
- Commercial photography,

- Aerial mapping and charting
- Surveillance
- Surveying forests
- Tracking forest wildfires

During the design process, it has been found out that aerial inspection is common for inspecting Telecommunications towers and there is a possible market in worldwide (specially south America) for civil operations such as surveillance and reconnaissance missions in fighting drug cartels and against guerrillas.

The two main types of UAVs in the commercial market are fixed-wing and multi-rotor. Both have them advantages and disadvantages including their suitability for certain applications. Fixed-wing UAVs normally have longer flight endurance capabilities while multi-rotors can provide for stable image capturing and easy vertical take-off and landing.

High demand in Aerial surveying and mapping, Aerial inspection of infrastructure, and terrain modeling of larger areas is expected to keep the market for fixed-wing UAVs buoyant.

By using RFP requirements and studying demands and operations in worldwide, some countries have been selected to being market targets. Mentioned countries are United States, Canada, Mexico, Brazil, Argentina, France, Germany, United Kingdom, Italy, China, India, and Russia.

3 Mission Analysis

3.1 Power line inspection mission analysis

Power Line surveillance mission's purpose is to avoid vegetation interference with power lines and determine power line's SAG, temperature, and also to detect tree species near the power lines, the condition of transmit towers, and growth of plants and trees to schedule clear corridors plan. Determine SAG, detect growth of plants and trees, and probability of vegetation interference can be done with LIDAR and determining power line's temperature and detection of tree species and transmit tower condition can be

done with use of EO/IR cameras. To get best results of LIDAR sensor (that is the main purpose of the request for proposal) it is important for an aircraft to maintain a certain speed relative to the ground.

Power line Location and its height (AGL) in different environment has been studied to determine the vehicle safe distance from power lines. This distance from power lines (optimum altitude) has been determined with considering danger zone (Table 3-1) and operating range of RIEGL miniVUX-1 UAV (260 ft.) and 14 CFR PART 107 rules "The altitude of the small unmanned aircraft cannot be higher than 400 feet above ground level". Results of this calculations is shown in Table 3-2.

Table 3-1: Danger Zone for Work Purposes

Power Line Voltage	**Personnel and equipment**	**Cranes and Derricks**	**Travel under or near Power Lines (on construction Sites, no load)**	
	(29 CFR 1910.333 and 1926.600)	(29 CFR 1926.1407,1408)	(29 CFR 1926.600-Equipment)	(1926.1411 – Cranes and Derricks)
0-750 volts	10 feet	10 feet	4 feet	4 feet
751-50000 volts	10 feet	10 feet	4 feet	6 feet
69000 volts	11 feet	15 feet	10 feet	10 feet
115000 volts	13 feet	15 feet	10 feet	10 feet
138000 volts	13 feet	15 feet	10 feet	10 feet
230000 volts	16 feet	20 feet	10 feet	10 feet
500000 volts	25 feet	25 feet	16 feet	16 feet

Table 3-2: Optimum Altitudes Considering Different Transmission Towers

Transmission tower	Height Range (ft.)	Optimum altitude (ft.)
66kV	92	160
132 kV	138-92	161
110 kV	90	160
150 kV	108	160
400 kV	148-180	192-225
220-kV single-circuit H-frame TSP	55-200	160-228
220-kV single-circuit TSP	70-200	160-228
220-kV double-circuit TSP	70-200	160-228
220-kV double-circuit LST	110-200	160-228
500-kV double-circuit LST	150-215	195-255
500-kV single-circuit LST	80-200	160-245

Designing missions has been done by studying Environments that power transmission lines, gas pipeline transport, railways, and jungles in which countries that decided to be market targets. Then some information has been gathered about their climate, and arrangement of linear infrastructures and by using this information, designing the mission has been begun. A description of the missions is shown below.

In case of using car top launch method for launching the vehicle, before the beginning of the mission, wind direction will be determined and set the truck with it. WAAPI UAV has to set elevator before the launch. After launching the vehicle, WAAPI UAV perform loiter to set itself with wind direction. Mission planning will be done by UGCS software. At the end of the mission, another loiter will be performed to determine wind direction for landing. If sufficient runway isn't accessible, WAAPI use parachute for a safe recovery.

To avoid using WAAPI in non-civil missions (such as suicide attack or using it in battlefield), WAAPI UAV will check its mission (that planned in UGCS) and in case of using for non-civil missions will be land automatically.

Mission: Cover 100 linear miles of power transmission lines in one day. The truck will position itself at the center of this linear extent at the beginning of the mission such that the aircraft must fly 50 miles in either direction before returning to the midpoint in this mission, power transmission lines will be inspected twice and in result of that, this mission has more accuracy. Mission details is shown in Table 3-3 and Figure 3–1.

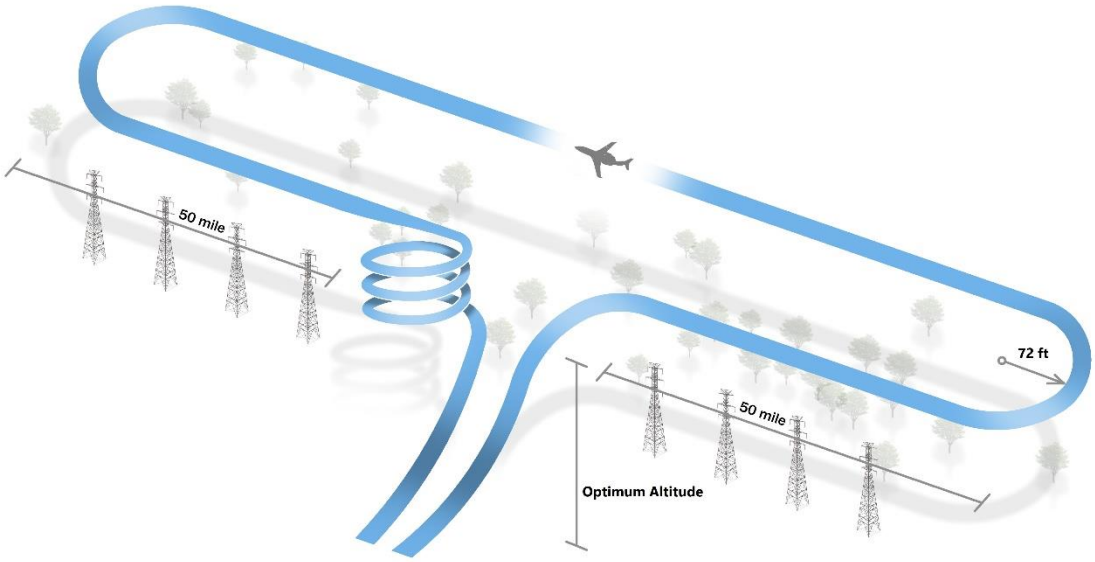

Figure 3–1 1st mission profile

Table 3-3 Summary of flight segments of WAAPI (1st mission profile)

	Segment	Description
1	Takeoff, car top launch	Take-off distance 150 ft. Take-off and launch Speed 62.5 ft./s
2	Climb	at max power
3	Cruise accelerates	Range=25miles, Max cruise speed=82 ft./s, Optimum altitude
4	Cruise decelerates	Range=25miles, Min cruise speed=63 ft./s, Optimum altitude
5	Turn	Turn Radius= 72 ft., Turn speed=63ft/s G Load=2
6	Cruise accelerates	Range=25miles, Max cruise speed=82 ft./s, Optimum altitude
7	Cruise decelerates	Range=25miles, Min cruise speed=63 ft./s, Optimum altitude
8	Cruise accelerates	Range=25miles, Max cruise speed=82 ft./s, Optimum altitude
9	Cruise decelerates	Range=25miles, Min cruise speed=63 ft./s, Optimum altitude
10	Turn	Turn Radius= 72 ft., Turn speed=63ft/s G Load=2
11	Cruise accelerates	Range=25miles, Max cruise speed=82 ft./s, Optimum altitude
12	Cruise decelerates	Range=25miles, Min cruise speed=63 ft./s, Optimum altitude
13	Loiter	5 minutes
14	Descend	
15	Landing / Recovery	Landing distance=280 ft., Recovery by parachute Rate-of-Descent 16.4 ft./s

In 2nd mission, power transmission lines with 100 miles of length will be inspected, with considering payload's field of view, each line will be inspected twice.

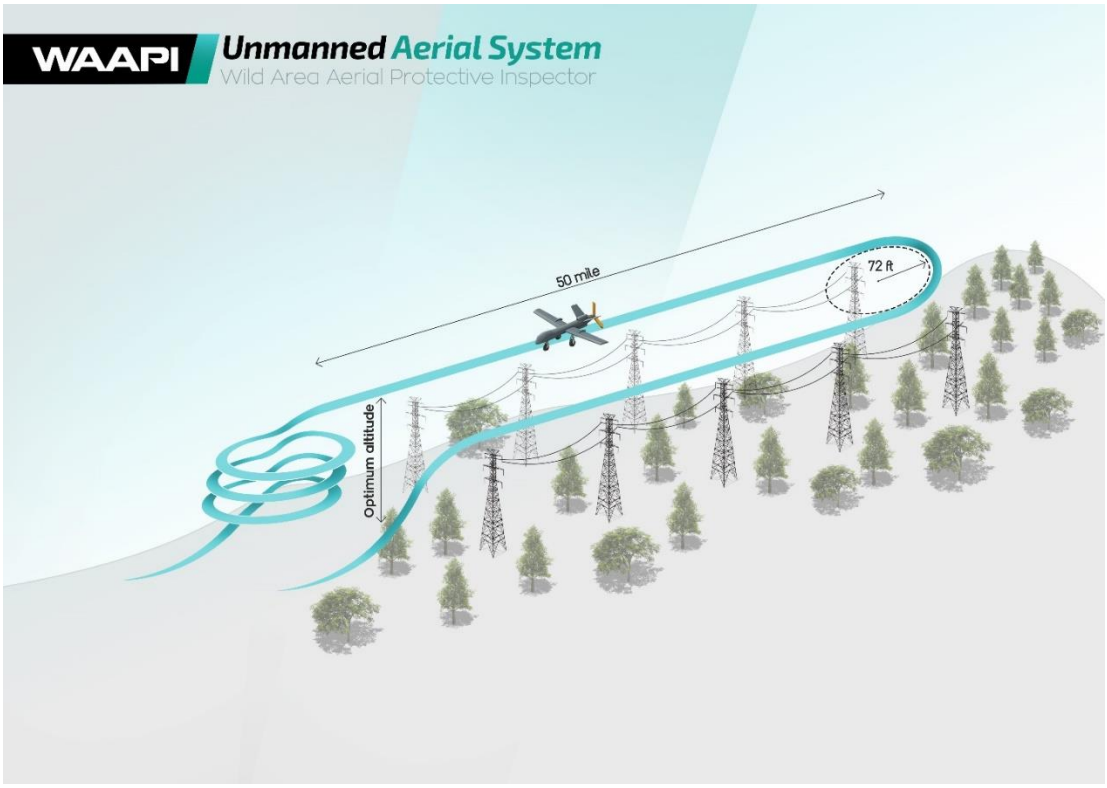

Figure 3–2 2nd mission profile

Table 3-4: Summary of WAAPI's flight segments (2nd mission profile)

	Segment	Description
1	Takeoff, Launch	Take-off distance 150 ft. Take-off and launch Speed 62.5 ft./s car top launch
2	Climb	at max power
3	Cruise accelerates	Range=50miles, Max cruise speed=82 ft./s, Optimum altitude
4	Cruise decelerates	Range=50miles, Min cruise speed=63 ft./s, Optimum altitude
5	Turn	Turn Radius= 72 ft., Turn speed=63ft/s G Load=2
6	Cruise accelerates	Range=50miles, Max cruise speed=82 ft./s, Optimum altitude
7	Cruise decelerates	Range=50miles, Min cruise speed=63 ft./s, Optimum altitude
8	Loiter	5 minutes
9	Descend	
10	Landing / Recovery	Landing distance=280 ft., Recovery by parachute Rate-of-Descent 16.4 ft./s

3rd mission has been designed to inspect power transmission lines that placed in sloped areas, in first phase of mission flown 50 miles to determine slope ratio of linear infrastructure, then in final phase aircraft will inspect power transmission lines. A conceptual picture of this mission is shown in Figure 3–3 and its details can be found in Table 3-5.

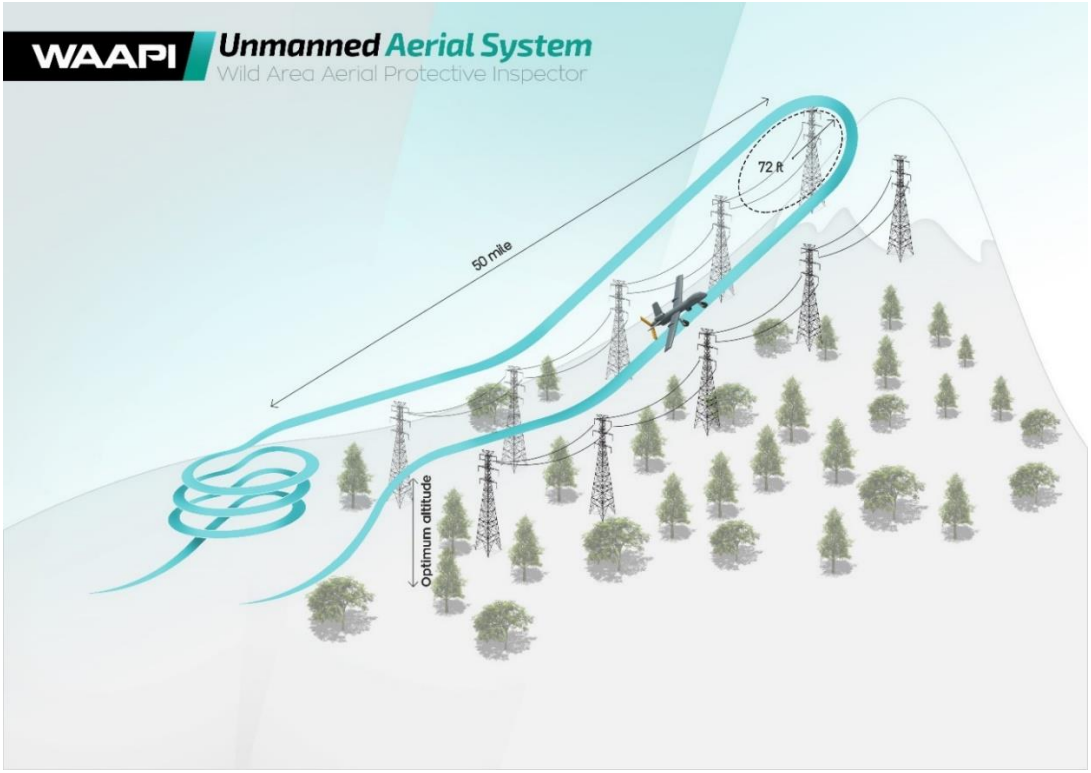

Figure 3–3 3rd mission profile

Table 3-5: Summary of WAAPI's flight segments (3rd mission profile)

	Segment	Description
1	Takeoff, Launch	Take-off distance 150 ft. Take-off and launch Speed 62.5 ft./s
2	Climb	at max power
3	Cruise climb accelerates	Range= 25 miles, Max cruise speed=82 ft./s, Optimum altitude
4	Cruise climb decelerates	Range= 25 miles, Min cruise speed = 63 ft./s, Optimum altitude
5	Turn	Turn Radius= 72 ft., Turn speed=63ft/s G Load=2
6	Cruise descend accelerates	Range = 25 miles, Max cruise speed = 82 ft./s, Optimum altitude
7	Cruise descend decelerates	Range = 25 miles, Min cruise speed = 63 ft./s, Optimum altitude
8	Loiter	5 minutes
9	Descend	
10	Landing / Recovery	Landing distance=280 ft., Recovery by parachute Rate-of-Descent 16.4 ft./s

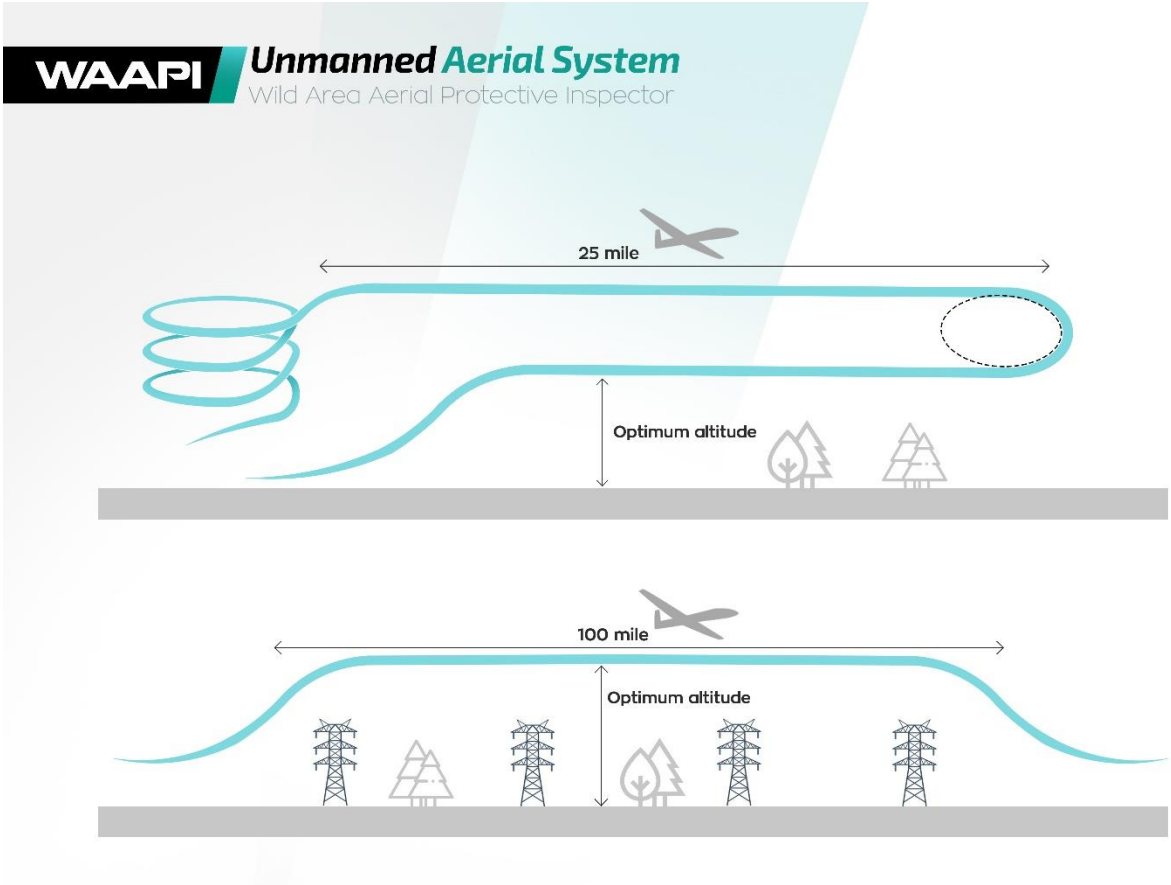

Figure 3–4 4th (up) and 5th mission (down)

For the missions that has been set to tracking forest wildfires, aerial mapping, charting, and surveying forests, 5th mission has been designed. A conceptual picture of this mission is shown Figure 3–4 and its details can be found in Table 3-6.

Table 3-6: Summary of WAAPI's flight segments (4th mission profile)

	Segment	Description
1	Takeoff, Launch	Take-off distance 150 ft. Take-off and launch Speed 62.5 ft./s car top launch
2	Climb	at max power
3	Cruise accelerates	Range= 25 miles, Max cruise speed= 82 ft./s, Optimum altitude
4	Loiter	10 hours
5	Cruise decelerates	Range = 25 miles, Min cruise speed = 63 ft./s, Optimum altitude
6	Loiter	5 minutes
7	Descend	
8	Landing / Recovery	Landing distance=280 ft., Recovery by parachute Rate-of-Descent 16.4 ft./s

When aircraft encounter a headwind (head wind>stall speed) that can make WAAPI to stall, WAAPI avoid to turn and will be recover by passing 100 miles. A conceptual picture of this mission is shown Figure 3–4 and its details can be found in Table 3-7.

Table 3-7: Summary of WAAPI's flight segments (5th mission profile)

	Segment	Description
1	Takeoff, Launch	Take-off distance 150 ft. Take-off and launch Speed 62.5 ft./s car top launch
2	Climb	at max power
3	Cruise	Range= 100 miles, Max cruise speed= 82 ft./s, Optimum altitude
4	Recovery	Recovery by parachute Rate-of-Descent 16.4 ft./s

3.2 Concept of operation

The concept of operations detailed in this section informs the mission requirements for the WAAPI. The operational strategy of the aircraft was conceived by considering the important features of an aircraft deployed for linear infrastructure inspection. Before deployment for communication support, the disassembled (without wing, tail, and booms) aircraft shown in Figure 3–5 is mount on 2018 F-150 and ready for shipment. Two containers hold the ground station equipment and wing, tail, and booms part. The whole system will be assembled by two ground crew members.

Figure 3–5 Disassembled aerial vehicle

Launching UAV will be performed by two methods, in case of access to sufficient runway (with 150 ft. of length) in concrete, wood, asphalt, hard turf, and grass surfaces. In case of inaccessibility to suitable runway (for example: soft ground) car top launch method will be used to launch the WAAPI.

The launch mechanism shown in Figure 3–6 is a metal frame used to support the UAV on the roof of a launch vehicle, pick-up truck, to allow for a vehicle-assisted launch. The ground team performs avionics and systems checks and fills the fuel tanks.

Figure 3–6 Car top launch parts

If case of using car top launch method to launching the WAAPI, metal frame (Figure 3–6) will be used and in 500 ft. (The aircraft launch requires less than 500ft.) after start launching, when rotation speed is

reached, Autopilot performs a pull-up maneuver to allow the aircraft to separate from the vehicle. After takeoff, the ground-based pilot transfers control authority of the aircraft to the autopilot system. The aircraft autonomously climbs to the loiter altitude of 260 ft. to determine dominant wind direction in order to set the mission.

The aircraft then cruises to the communication support zone. The aircraft's payload provides high-speed data acquisition using echo signal digitization and online waveform processing then communication link will be provided between ground units that are line of sight and capable beyond line-of-sight (BLOS) in difference environment from each other. Communication between the aircraft and its operators is maintained through a satellite-based Internet system, which allows operators to receive telemetry data regarding the aircraft's systems. After landing, the ground team performs the necessary maintenance.

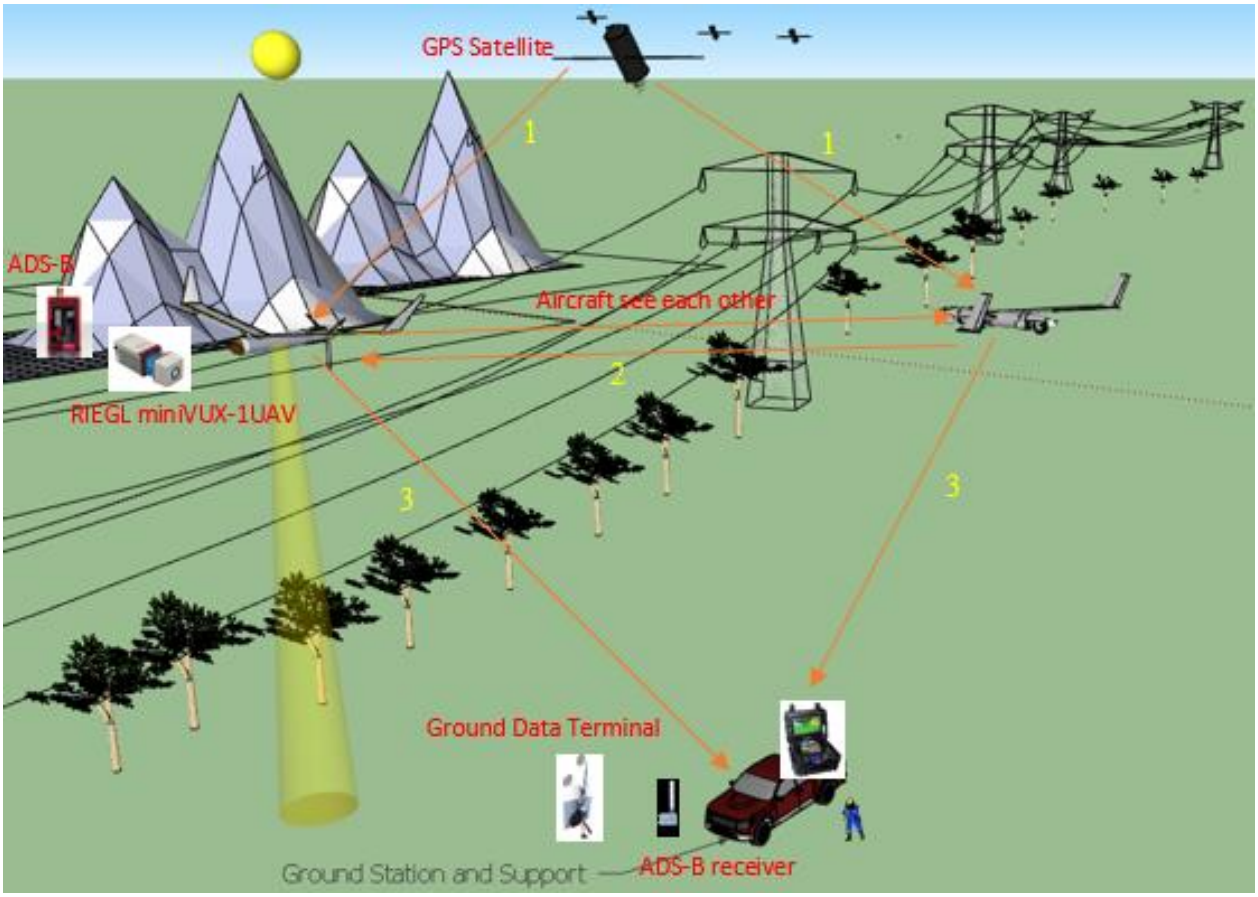

Figure 3–7 Concept of operation

- GPS satellites provide location information to ADS-B equipped aircraft.
- ADS-B equipped aircraft transmit altitude, speed, and velocity information to another ADS-B equipped aircraft and ADS-B ground stations.
- ADS-B ground receive stations provide aircraft location back to other aircraft, as well as air traffic control centers.
- The RIEGL minivux-1UAV makes use of RIEGL's unique Waveform-LIDAR technology, allowing echo digitization and online waveform.

4 Constraint Analysis

Constraint analysis is a method for defining a solution space such that all design points within that space allow the design to meet specific performance requirements. The design points are defined by combinations of wing loading, W_{To}/S, and takeoff power loading P/W_{To}.

4.1 Drag Polar

The drag polar is useful in characterizing to design an UA because it is dependent on distinguishing Features including the weight of the UA, the airfoil used, gimbal, landing gear, and the shape of the fuselage. Also, important is the fact that the drag polar can be used to calculate other performance parameters. One form of the drag polar is described by the Equation 4-1.

$$\text{Equation 4-1} \quad C_D = C_{D0} + K_2 C_l + K_1 C_l^2$$

If the assumption is made that minimum drag occurs at zero lift, the drag polar can be expressed as:

$$\text{Equation 4-2} \quad C_D = C_{D0} + K C_l^2$$

WAAPI's Efficiency Factor, e, is determined using Eqn. x where AR is the aspect ratio of the wing. [1]

$$\text{Equation 4-3} \quad e = 1.78(1 - .045AR^{.68}) - .64$$

The WAAPI coefficient (K) is used to simplify the equation can be calculated as:

Equation 4-4 $K = \frac{1}{\pi ARe}$

WAAPI's Basic aerodynamic coefficients can be found in Table 4-1.

Table 4-1: Airfoil database for small UAVs

Parameter	Value
C_{D0}	0.0418
$C_{L\ TO}$	1.011
$C_{L\ Lan}$	1.35

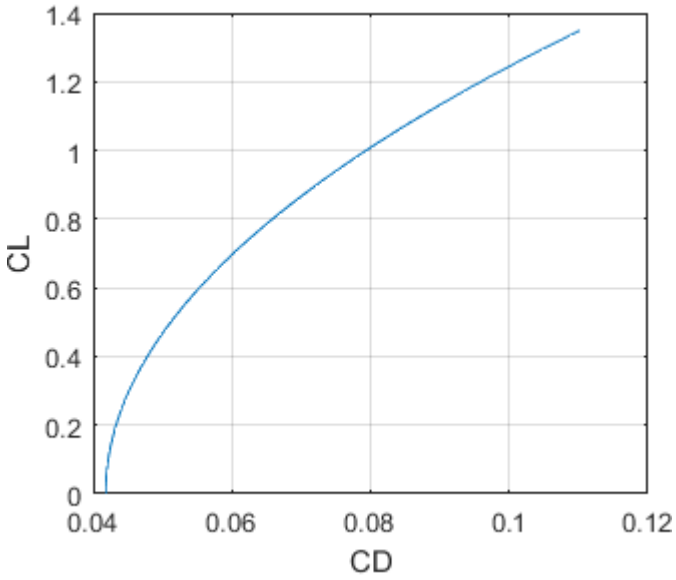

Figure 4–1 Drag Polar

4.2 Sustained Turn Constraint

In order to minimize turn radius, velocity needs to be minimized and the load factor maximized. Maximizing turn rate also requires that velocity be minimized and the load factor maximized

In beginning and finalizing phase of mission, WAAPI perform loiter to check the wind direction and speed, to set the mission, to reach this purpose it is desired to perform loiter in less radius and avoid wasting

fuel. To reach this goal, considered loiter speed has been decreased (with considering stall limit and V-N diagram)

The equations of flight for a steady level turn used to derive a relationship between the load factor and thrust available. [2]

Equation 4-5 $$\frac{T}{W} = \frac{q\, C_{D0}}{W/S} + \frac{W}{S}\left(\frac{n^2}{q\pi Ae}\right)$$

4.3 Take-Off Ground Run Constraint

By analyzing market, typical locations for operation has been detected and accessible runway distance and ground friction constant of operating location has been assumed. This assumption has been made to give the WAAPI capability of taking off and landing from unimproved dirt roads and clearings (dirt, grass)

The equations that used to determine thrust to weight ratio required for a target ground run distance to take off and landing has been shown below.

Equation 4-6 $$\frac{T_{SL}}{W_{TO}} = \frac{1.44\,\beta^2}{\alpha\,\rho\,g S_{TO}\,C_{Lmax}}\left(\frac{W_{TO}}{S}\right) + \left(\frac{q\,C_{D0}}{\beta\left(W_{TO}/S\right)}\right) + \mu$$

Equation 4-7 $$\frac{P}{W_{TO}} = \frac{T_{SL}}{W_{TO}}\left(\frac{V_{TO}}{550\,\eta_P}\right)$$

Equation 4-8 $$V_{TO} = 1.2V_{Stall}$$

Equation 4-9 $$\frac{W}{S} = \frac{\rho\, g\, \mu\, C_{Lmax} d_{land}}{1.68\,\beta}$$

Table 4-2 Values for constraint equation during takeoff and landing

Parameter	Unit	Value
Takeoff distance	ft.	150
Landing distance	ft.	250
μ_{TO}		0.1
$\mu_{Landing}$		0.3
V_{TO}	knots	37
$V_{Approach}$	knots	35

4.4 Rate of Climb Constraint& Flight Envelope

The climb performance of an aircraft and its variation with altitude is the result of a complex web of interactions between the aerodynamics of lift generation and the response of its power plant to varying atmospheric conditions and airspeed. Maximum rate of climb is 500 ft/min. The maximum rate of climb ROC_{max} is the rate of climb that results from maximum thrust. For small angles, this is given by:

Equation 4-10 $$ROC_{max} = \left(\frac{T_{max}-D}{W}\right)V$$

Climb analysis was determined, using Equation 4-11. [2]

Equation 4-11 $$\frac{T}{W} = \frac{ROC}{V_{Climb}} + 4\frac{q_{climb}C_{D0}}{w} + k\frac{W/_S}{q_{Climb}}$$

4.5 Stall Speed

To determine stall speed of WAAPI, weather of operational areas and type of operation (power transmission line inspection) has been considered. It is assumed that average wind speed will be 20 knots. To perform the mission with high reliability, stall speed will be calculated with 1.2 for safety factor and resulted stall speed will be 31 knots.

Equation 4-12 is the wing loading required for Stall Speed [2]

Equation 4-12 $$\frac{W}{S} = q_{app} C_{Lapp}$$

4.6 Max Cruise Airspeed

Important factors to determine max speed include: lower operating cost by minimizing duration of operation to surveying linear infrastructure and power lines accurately. To survey power transmission lines, it is required to:

- First: Check the linear infrastructure with maximum speed and then
- Check them with lower speed and more accuracy

This consideration results 54 knots for maximum cruise airspeed.

The required thrust to weight ratio T⁄W for max cruise airspeed as a function of the wing loading W⁄S can be calculated as:

Equation 4-13 $$\frac{T}{W} = \frac{C_{D0} q_{max}}{W/S} + \left(\frac{W}{S}\frac{K}{q_{max}}\right)$$

4.7 Matching for Sizing Requirements

By running MATLAB code and comparing the rivals (Penguin B and C, ScanEagle, Textron Aerosonde) design points determined a design point for power loading and wing loading. Figure 4–2 shows this design point in terms of a specified power loading and wing loading value. [2]

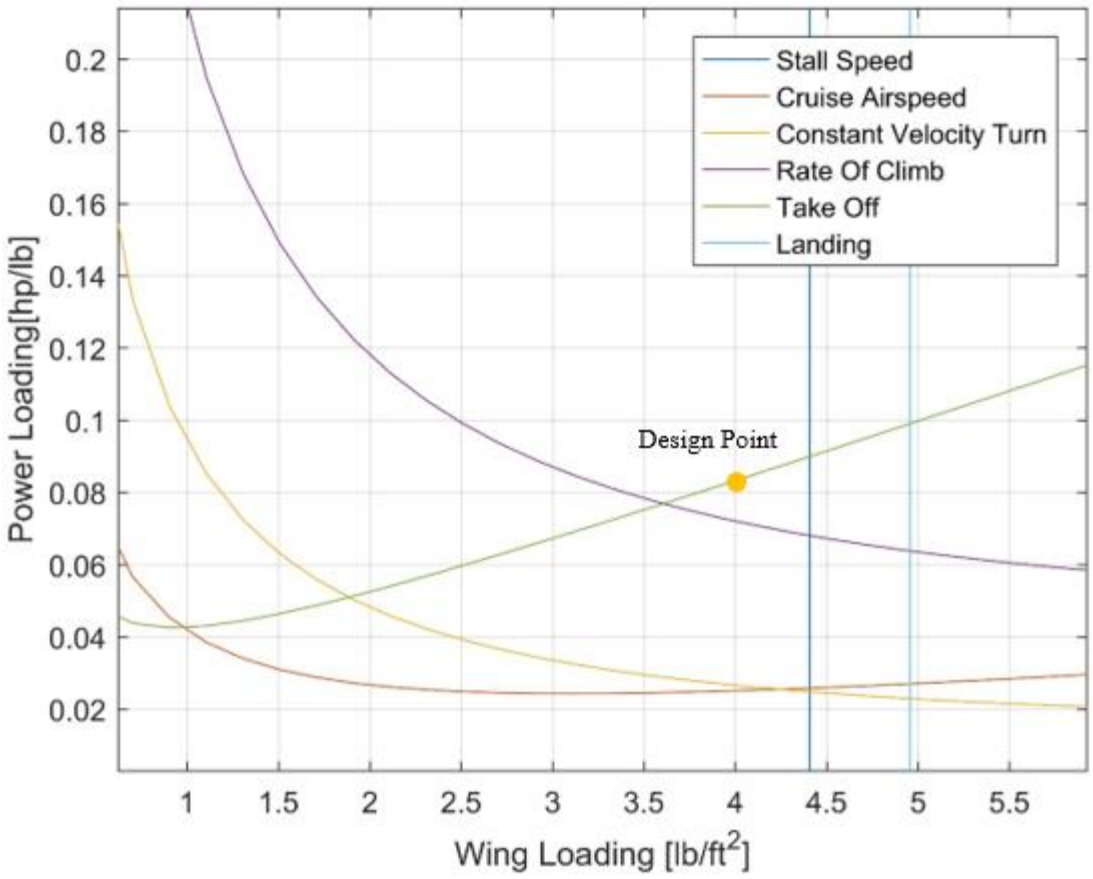

Figure 4–2 Results of aircraft constraint analysis

Table 4-3 shows the optimum design point data.

Table 4-3 Power loading and wing loading data

Power Loading	0.086 (Hp/lb)
Wing Loading	4 (lb/ft^2)

5 Sizing Analysis

Weight sizing is a process to estimate takeoff weight (including fuel) of an aerial vehicle for a specified mission. This process has been done for designed missions and aircraft's MTOW will be computed by the most critical mission. The general technique to estimate the MTOW is as follows: the aircraft weight is broken into several parts. Some parts are determined based on statistics, but some are calculated from performance equations. The MTOW is broken into three elements:

1. Payload weight ($W_{Payload}$).
2. Fuel weight (W_{Fuel}).
3. Empty weight (W_{Empty}).

Equation 5-1 $$W_{TO} = W_{Pay} + W_{Fuel} + MF_{Empty}W_{TO}$$

A process for preliminary weight sizing show in Figure 5–1.

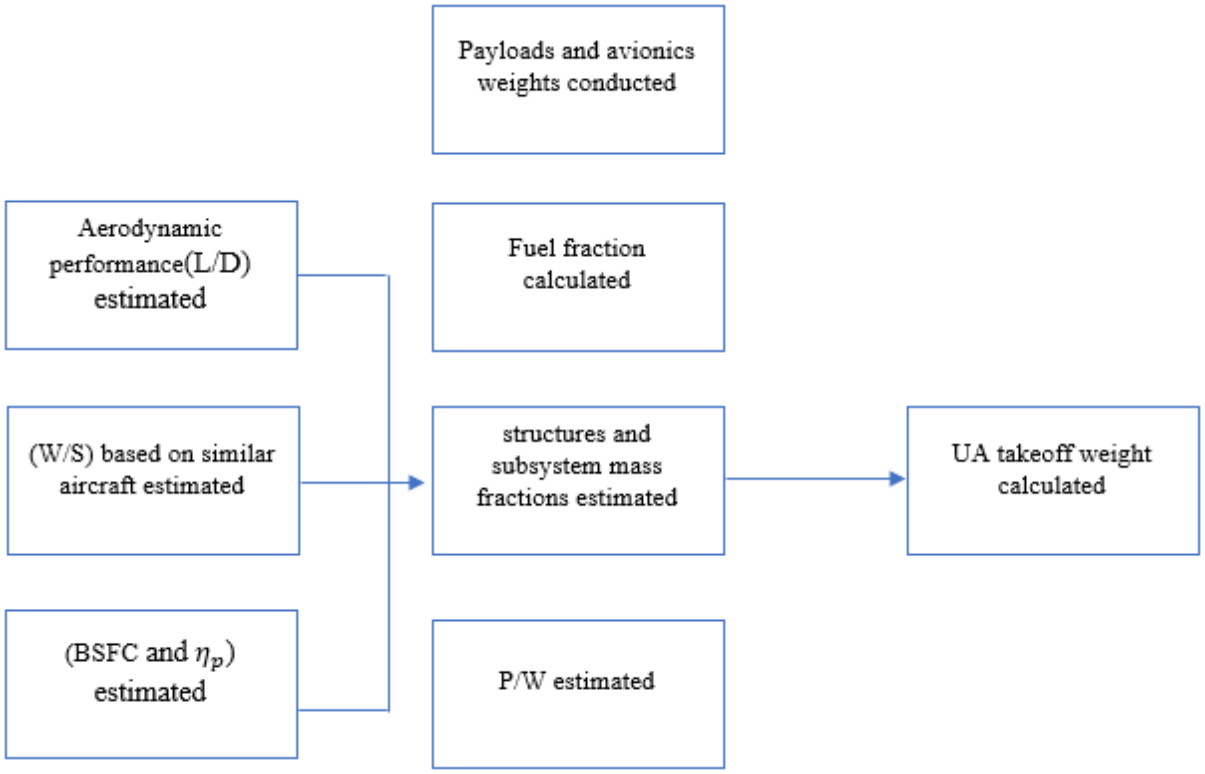

Figure 5–1 Preliminary weight sizing process

5.1 Payload Weight

According to RFP, the baseline payload is RIEGL miniVUX-1UAV weighing 4.4lb. Lt965R has been chosen as high-resolution still camera weighing 0.4 lb. another optional payload is a Long Wave Infrared fixed camera for detecting transmission line temperature and find fire, FLIR TAU-2-640 has been chosen to perform this mission and its weight is 0.15 lb.

5.2 Fuel Weight

The fuel fraction and weight equations derived from the Breguet equation for cruise and loiter, used to find the gross weight, are shown in Equation 5-2 and Equation 5-3 respectively.

Equation 5-2 $$\frac{W_i}{W_{i-1}} = [\frac{-RC_{bhp}}{550\eta_p(L/D)}]$$

Equation 5-3 $$\frac{W_i}{W_{i-1}} = [\frac{EVC_{bhp}}{550\eta_p(L/D)}]$$

In these equations R stand for range, E stands for endurance, C_{bhp} stands for the specific fuel consumption for propeller aircraft. η_p stands for the propeller efficiency. The aircraft weight is calculated throughout the mission. For each segment, the aircraft weight is reduced by fuel consumption. Total fuel burned is calculated throughout the mission and found by summing the weight fractions from each flight segment in Equation 5-4.

Equation 5-4 $$W_{fuel} = 1.06(\sum_i^x W_{fi})$$

5.3 Empty Weight

The empty weight mass fraction is the ratio of the empty weight W_{Empty} to W_{TO} in Figure 5–2 [3] shows this mass fraction parameter for fixed-wing and helicopter unmanned aircraft across several orders of magnitude in W_{TO}.

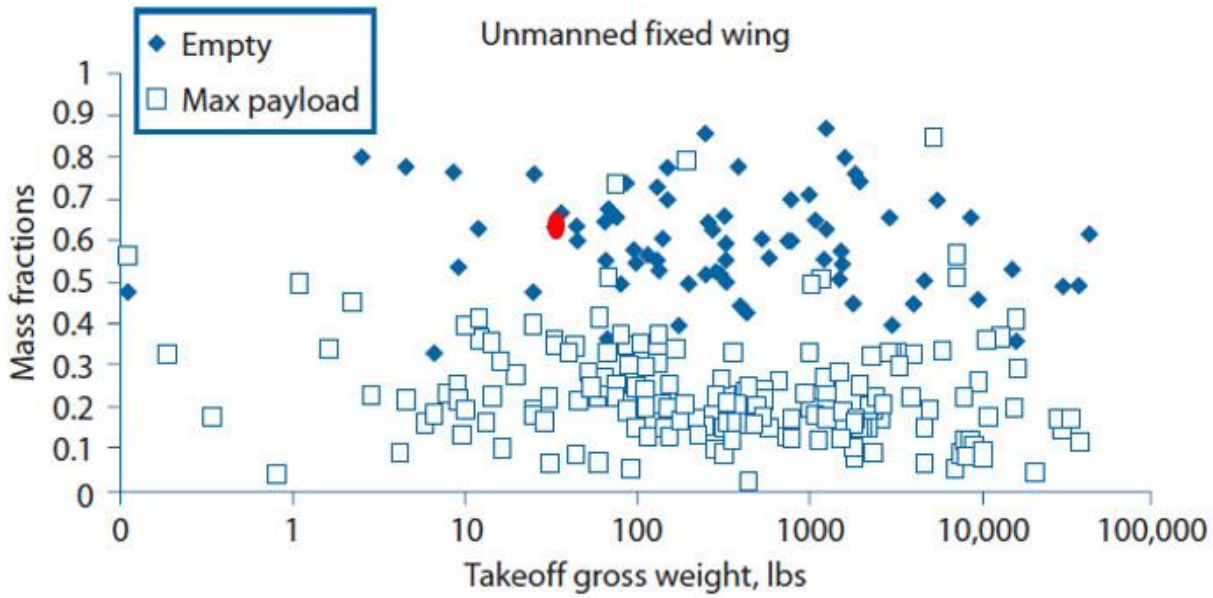

Figure 5–2 Empty and maximum payload mass fractions for fixed-wing unmanned aircraft

Equation 5-5 $$MF_{Empty} = \frac{W_{Empty}}{W_{TO}}$$

By study the SUAS's takeoff weight database and using Figure 5–2 as a reference, $MF_{Empty} = 0.66$ has been chosen to use in calculations.

Results of weight sizing process have been shown in Figure 5–1.

Table 5-1 Weight sizing results

Total Aircraft Takeoff weight	**36 lb.**
Empty Weight	23.7 lb.
Fuel Weight	2.3 lb.
Payload Weight	10 lb.
Power Required	3.1 Hp
Wing Area	9 ft^2

6 Unmanned-Aircraft Geometry and Configurations

6.1 Configuration Drivers

In this section, the process of selecting configuration after initial sizing will be presented. This process is formed based on extracted requirements from RFP and designed missions. Selected configuration is result of design approaches such as transportability, maintainability, damage tolerance, more reliability and lower manufacturing cost. Additional information on the individual components of either aircraft may be explained in more detail in other sections of the report.

6.2 Wing System Configurations

Conventional configurations can yield very high aerodynamic efficiency in terms of lift-to-drag ratio (L/D) and endurance parameter. The wing was designed for lifting capability or aerodynamic efficiency without imposing pitch trim requirements on the wing. A higher L/D is desirable and with 10 hours of endurance, vehicle has an acceptable performance.

With the tail providing trim, the main wing is able to generate high lift coefficients. No surfaces ahead of the wing generates undesirable downwash on the wing or a turbulent wake.

By designing a wing with no taper, manufacturing cost is lower than other alternatives (for example tandem wing and canard), the WAAPI conventional wing results in lower weight in comparison to tandem wing or canard, and because of lower quantity of components in this configuration, maintenance cost is also decreased. The canard configuration is relatively rare for UAS applications because there are no aerodynamic advantages over the conventional configuration and it has more parts than a flying wing .If the wing were to stall first, the loss of lift behind the center of gravity would cause the nose to rise further and make unstable pitch break increase.

Tandem wing configuration like a canard, the forward wing produces a downwash field on the rear wing. This generates higher induced drag on the aft wing. It has a lower aerodynamic efficiency relative to a

conventional wing configuration for an equivalent wetted aspect ratio. The tandem wing configuration might experience poor stall behavior.

Installation of landing gear on a flying wing is also difficult. This exposes the downward facing camera to the risk of damage as every landing is a belly landing.

Flying wing configuration is less stable (more sensitive to canter-of gravity location) as well as the wing's high stall speed makes it difficult to achieve minimum flying airspeed with a car top launch. Installation of landing gear on a flying wing is also difficult.

In case of mal-functioning retractable gimbal actuator, the downward facing camera to the risk of damage in landing.

Table 6-1 Configuration table of merit analysis

	Weighting	**conventional**	**Flying Wing**	**Canard**	**Tandem**
Aerodynamic Performance	20	19	17	14	12
Controllability	17	16	9	13	13
Ease of Manufacturing	16	13	10	9	6
Maintainability	15	10	13	7	5
weight	68	58	49	43	36

6.3 Fuselage System Configurations

Designing fuselage is began with fitting all the components that is supposed to place inside it. Some requirements have been considered such as less drag, ease of boarding, swap out a failed component, access to fuel tank, and engine (for maintenance and inspection). Accessible areas have been shown in Figure 6–1.

Figure 6–1 Fuselage accessible areas

Also, in fuselage design it has been considered to remove optional payload (EO/IR camera) easily, and when landing on the ground as well as in the case of emergency recovery optional payload goes inside the fuselage by an actuator. To make the main payload's mission feasible, a part of fuselage made of glass.

6.4 Tail Configurations

Twin booms have the option of attached or disconnected tails, and this specification is helpful and make boarding easier. Boom attachment point increases the moment arm between the center of gravity and the tail aerodynamic center and therefore reduce the tail size required for a fixed tail volume coefficient.

The tail configuration selection for this aircraft compares Twin boom conventional, Twin boom H, Twin boom T and Twin boom inverted V designs. A twin boom inverted V, shown in Figure 6–2, was selected for the aircraft's tail. This configuration was selected because of several reasons.

Cost of building this tail is lower (cause of same shapes of it parts). And cause of less weight in V-tail configuration it needed less materials. For control surfaces (in tail), 4 electromechanical actuators has been

used (2 for each control surface) to make it more reliable. By using twin boom inverted V, number of parts that supposed to be assembled decreases and in result of that time for assembling WAAPI will decrease. Also it is easier for maintenance.

For connecting booms to tails, two holes (on each side) has been considered to replace each other in case of damaging on of them.

Figure 6–2 WAAPI UAV twin boom inverted V

Table 6-2 Tail configuration table of merit analysis

	Weighting	**Twin boom conventional**	**Twin boom H**	**Twin boom T**	**Twin boom inverted V**
Weight	20	10	10	10	20
Manufacturing Cost	15	8	8	8	12
Reliability	12	7	7	7	10
sum	47	25	25	25	42

6.5 Propulsion Integration

Placing the propulsion system in the aft of the fuselage prevent of creating very turbulent flow around the camera, extra vibrations and noise that will distort the picture.

7 Aerodynamic

7.1 Airfoil Selection

The process of selecting an airfoil began with the creation of a list of airfoils that are used on small UAs the most important criterions for selecting are High endurance/range, Easy to take-off, High Performance, and Easy to control. The airfoil set utilized in the selection are the ones performing at the operating Reynolds number. They are gathered from Table 7-1.

Table 7-1 Airfoil database for small UAVs

Airfoil	Thickness (%)	Camber (%)	Airfoil	Thickness (%)	Camber (%)
AG35	8.72	2.38	SD7036	9.20	2.79
S9000	9.01	2.37	SD7037	9.20	3.02
SD7035	9.19	2.55	SD7080	9.15	2.48

The airfoils analyzed by XFLR5 and data for drag polars, moments, and lift coefficient vs. angle of attack curves for the parameters received from the software's' analysis are compared with the experimental data. As the summary focus on an airfoil in the same Reynolds number (105–3×105) as the working condition of the fixed wing of SUAVs, it is for sure a precious reference for the fidelity analysis. The resulting comparisons are shown in Figure 7–1.

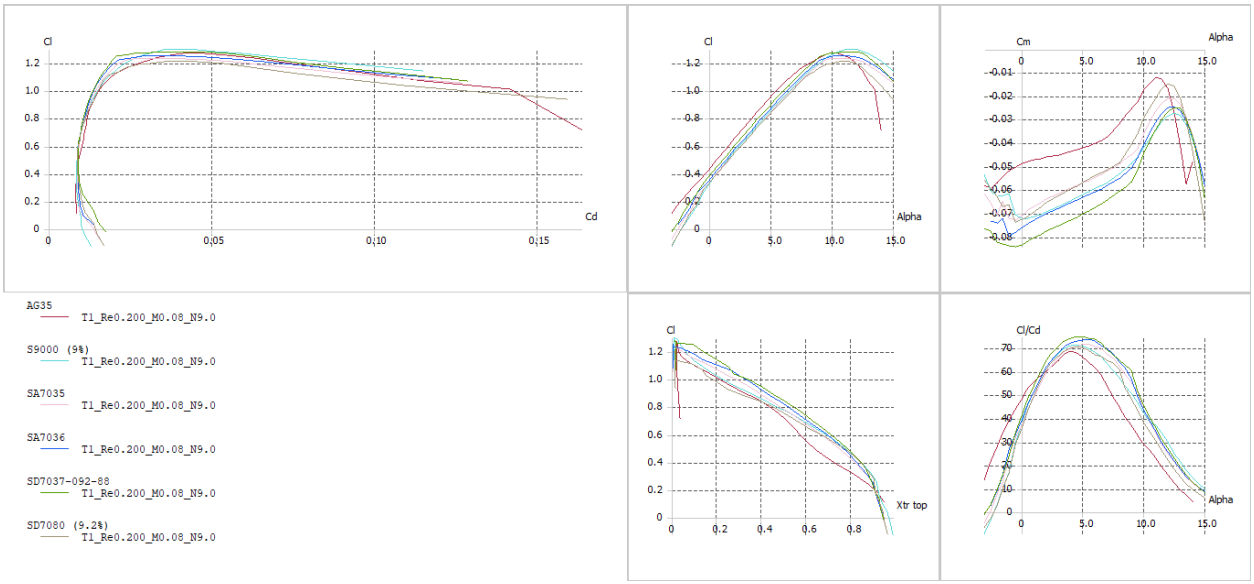

Figure 7–1 Airfoil parameter comparisons

Important parameters such as $C_{l\,max}$, L/D, C_{D0}, and C_{m0} of mentioned airfoils (table) has been studied in specified Reynolds ($3*10^5$). Among them, S9000 has highest $C_{l\,max}$ and also highest L/D (in 4.5 degrees of AOA). SD7037 airfoil has less C_m (-0.082) in the same Reynolds number and for comparison, S9000's C_m is -0.066. The lowest C_D in max AOA is belonged to S9000 airfoil too.

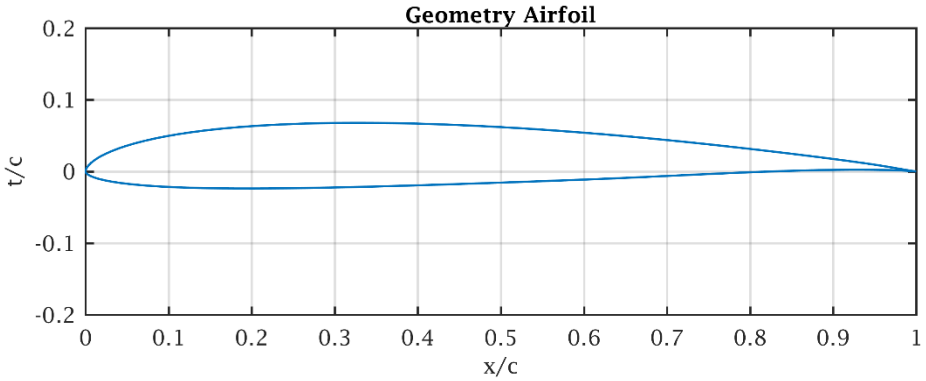

Figure 7–2 S9000 airfoil geometry

Table 7-2 S9000 airfoil parameters

$Max\ {C_l}/{C_d}$	Stall Angle	$Max\ C_l$	C_{m0}	${t}/{c}\ max$
81.2	11°	1.349	-.066	9.01%

7.2 Wing Geometry

With consideration of installing aircraft on top of the truck for transport it to operation area and considering its stall speed (31 knots) and truck may exceed the stall speed and make the wings fall off the aircraft. To avoid this situation, two scenarios have been studied:

1. The wing has three separate part that two of them can be removed and packed in a shipping suitcase.
2. Use a folding wing

Use a folding wing maybe avoid damage to aircraft in some cases, but doesn't ensure safety, but using the first method (removable wing) is more suitable and can ensure that aircraft's safety during transportation. The geometry of aircraft using removable wing can be found in Figure 7–3.

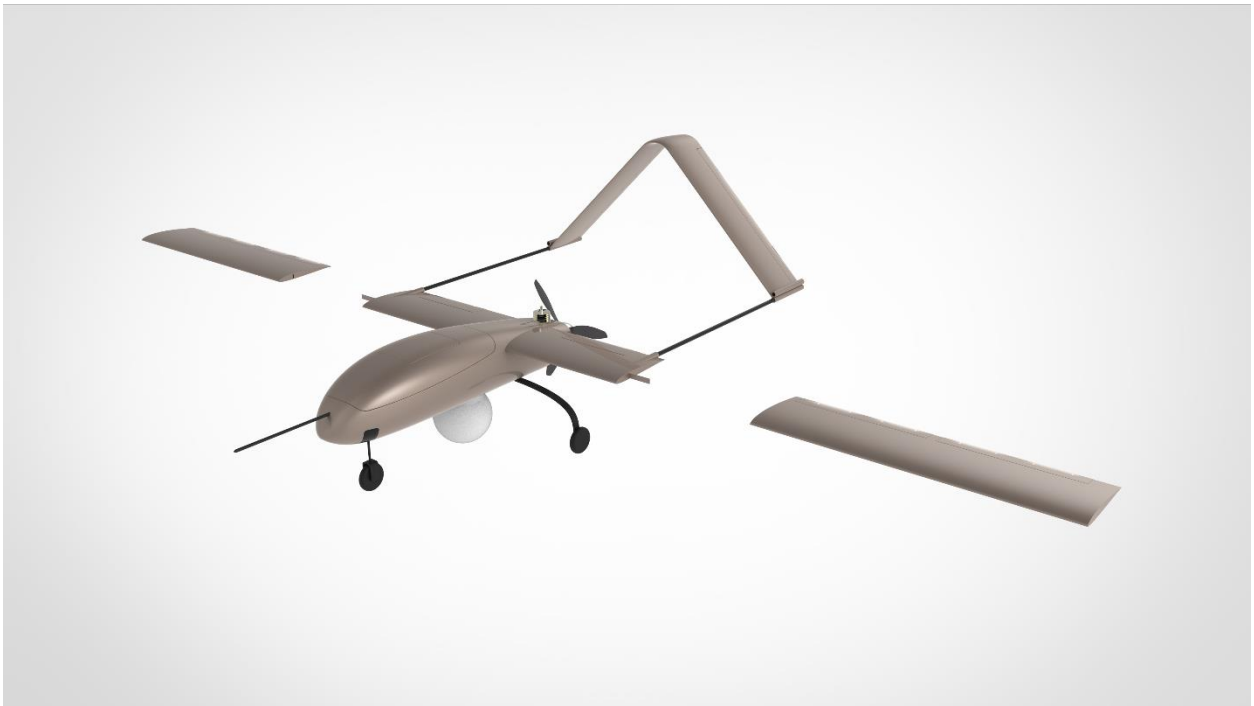

Figure 7–3 Removable wings

The sizing of the wing geometries for WAAPI began with a constraint analysis where the wing loading was Determined. The wing was sized using the method outlined in Roskam [1]. Then the taper and aspect

ratio has been determined by analyzing the effects of each parameter. Aircraft's wing has been modeled in XFLR5 software and result of this modeling has been shown in Figure 7–4.

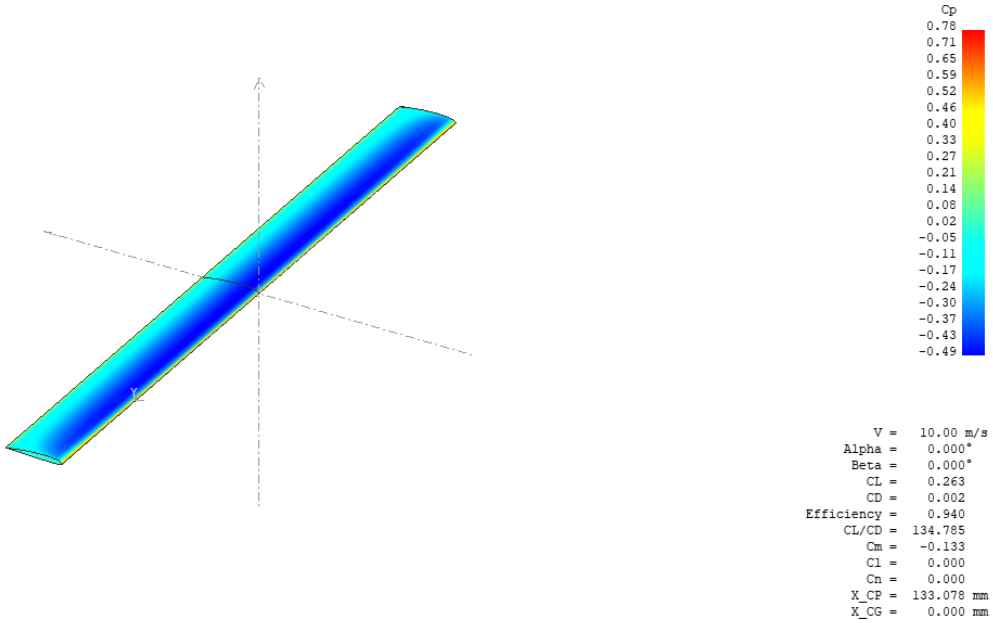

Figure 7–4 Aircraft's wing modeled in XFLR5 software

7.3 Flap Design

The flap deflection is considered as main and significant effects to the increment of maximum lift coefficient which indirectly influences on WAAPI takeoff, landing distance, and stall condition. To pass the 150 ft. takeoff distance the 25 degree flap angle is needed and in landing 35 degree flap angle is needed for the 280 ft. landing distance. Figure 7–5 shows the relative positions of the slotted flaps during takeoff and landing, with deflections listed in Table 7-3.

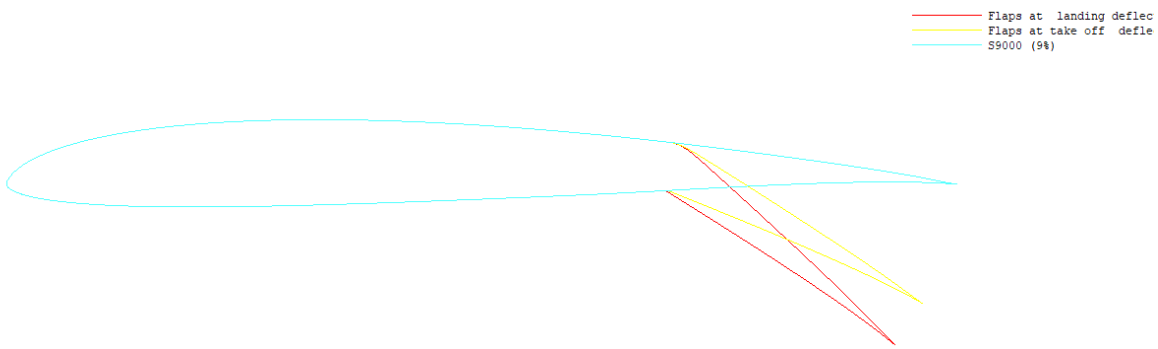

Figure 7–5: Flap Geometry

Table 7-3: Flap Geometric Parameters

Parameter	Value
Flap chord ratio	0.3
Flap deflection during takeoff	25 degrees
Flap deflection during Landing	35 degrees
Max flap deflection	40 degrees
Flap span ratio	0.18

8 Stability & Control

8.1 Tail configuration

There are a lot of good reasons to use an inverted V-tail. One of the big advantages of inverted V-tail designs is its stability in cross wind situations, in fact when facing a cross wind gust during landing the inverted V-tail will cause the airplane to pitch up as opposed to diving into the ground.

Figure 8–1 Tail configuration

8.2 Airfoil

Symmetric airfoils that are commonly used for the tails was examined. The NACA 0009 shown in Figure 8–2 airfoil was selected for tail because it was thinner than another symmetric airfoil. (S9000 (t/c) =9%, NACA 0009(t/c) =9.01 %,)

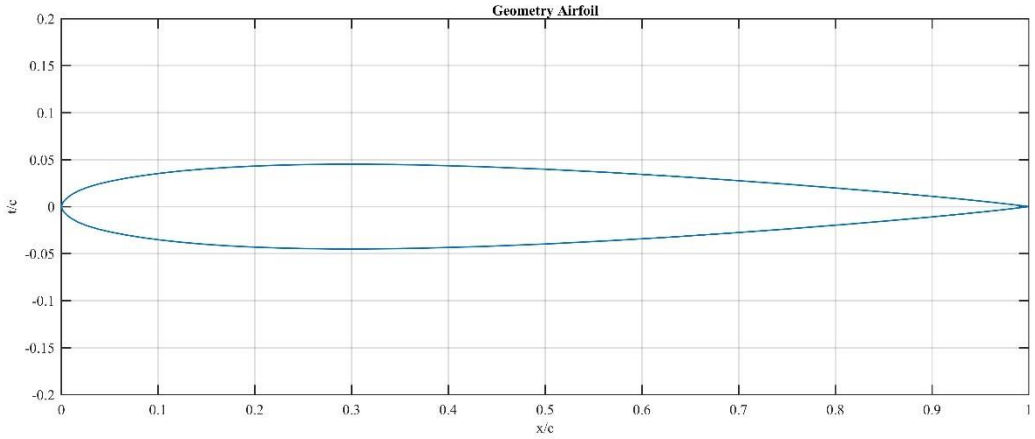

Figure 8–2 NACA 0009 Geometry Airfoil

Table 8-1 NACA 0009 airfoil parameters

$C_{d_{min}}$	C_m	$(\frac{L}{D})_{max}$	α_0(deg)	α_s(deg)	CL_α(1/rad)	(t/c) max
0.005	0	83.3	0	13	6.7	9%

8.3 Tail Sizing

In an inverted V tail aircraft, the two control surfaces of the tail work together to give both elevator and rudder response. For elevator control, both moving surfaces move up and down in the same direction. For rudder both surfaces move in opposite directions.

Areas for both horizontal and vertical tail is calculated according to Equation 8-1 and Equation 8-2 . So, both of them were sized using the method outlined in Sadraey. [4]

Equation 8-1 $S_H = S_T \times [\cos(\varphi)]^2$

Equation 8-2 $S_V = S_T \times [\sin(\varphi)]^2$

The geometric parameters of the tail are presented in Table 8-2.

Table 8-2 Tail geometric parameters

Parameter	Symbol	Value
Tail Area	S_T	3.18 ft^2
Horizontal Tail Area	S_H	1.59 ft^2
Vertical Tail Area	S_V	1.59 ft^2
dihedral angle	φ	45°
Volume Coefficient	$\bar{V}$	0.77
Chord	c	0.67 ft.
Span	b	2.30 ft.
Moment Arm	l	3.77 ft.

8.4 Control surface sizing

The control surfaces were sized using the method outlined by Sadraey [4]. Specifically, the geometric parameters were determined based on the method presented then modified to meet control authority and stability requirements for lateral and directional stability found in AVL. The deflection ranges of the control surfaces and general geometries are presented in Table 8-3.

Table 8-3 Deflection ranges of control surfaces

Control Surface	Deflection Range (degrees)	Chord Ratio	Span Ratio
Aileron	-25 - +25	0.22	0.54
Inverted V-tail	-30 - +30	0.3	0.9

8.5 Stability Derivatives

Control stability derivatives were extracted through the software AVL, as illustrated in Figure 8–3 for the WAPPI configuration. These extracted derivatives are shown in Table 8-4.

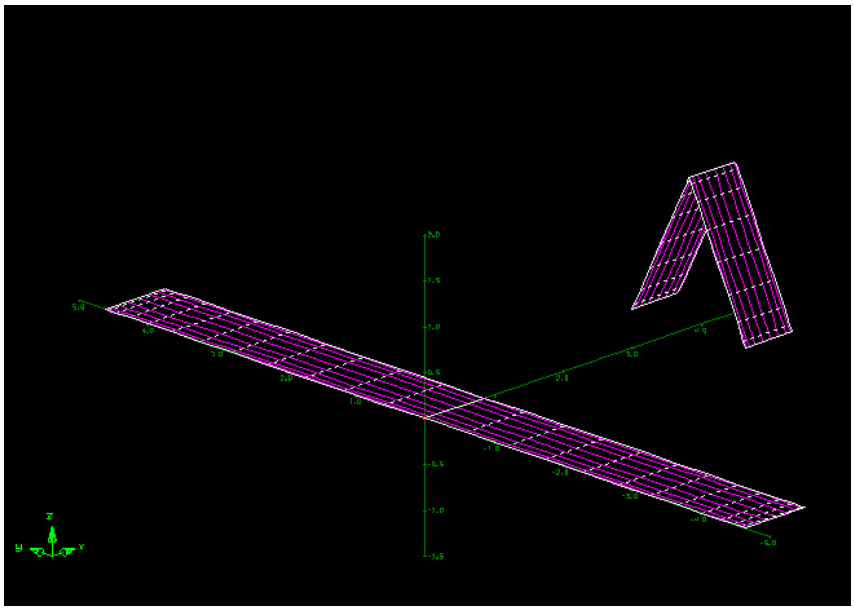

Figure 8–3 Control and stability analysis in AVL

Table 8-4 Stability derivatives of the WAAPI UAV

Symbol	Derivative	Value
Lift Coefficient		
C_{L0}		0.2614
$C_{L\alpha}$		6.1137
$C_{L\delta\varepsilon}$		0.7613
C_{Lq}		12.2757
Drag Coefficient		
C_{D0}		0.0604
$C_{D\delta\varepsilon}$		0.0218
$C_{D\delta\alpha}$		0.00025
$C_{D\delta r}$		0.0000
C_{Dq}		0.0000
Side Force Coefficient		
$C_{Y\beta}$		-0.0275
$C_{Y\delta\alpha}$		-2.35E-14
$C_{Y\delta r}$		0.2167
C_{Yp}		0.0000
$C_{Yr}r$		0.0000
Pitch Moment Coefficient		
C_{m0}		-0.1290
$C_{m\alpha}$		-0.6603
$C_{m\delta\varepsilon}$		-3.3145
C_{mq}		-14.4575
Roll Moment Coefficient		
$C_{l\beta}$		-0.0036
$C_{l\delta\alpha}$		0.9976
$C_{l\delta r}$		0.0089
C_{lp}		-1.8267

C_{lr}	-0.3874
Yaw Moment Coefficient	
$C_{n\beta}$	0.5693
$C_{n\delta\alpha}$	-0.1517
$C_{n\delta r}$	-0.2934
C_{np}	-1.8267
C_{nr}	-0.3874

8.6 Longitudinal Stability

The longitudinal static stability of the concept aircraft was evaluated using the method outlined in Roskam [1].

$$\begin{pmatrix} \dot{u} \\ \dot{w} \\ \dot{q} \\ \dot{\theta} \\ \dot{h} \end{pmatrix} = \begin{pmatrix} -0.0850 & 0.1094 & 0 & -9.8 & 0 \\ -0.3689 & -4.3476 & 22 & 0 & 0 \\ 0.4972 & -1.0214 & -2.951 & 0 & 0 \\ 0 & 0 & 1 & 0 & 0 \\ 0 & -1 & 0 & 25 & 0 \end{pmatrix} \begin{pmatrix} u \\ w \\ q \\ \theta \\ h \end{pmatrix} + \begin{pmatrix} 0.3377 & 32.5 \\ -11.7938 & 0 \\ -112.7973 & 0 \\ 0 & 0 \\ 0 & 0 \end{pmatrix} \begin{pmatrix} \delta_e \\ \delta_t \end{pmatrix}$$

Where the state variables $(u \;\; w \; q \; \theta \; h)$ refer to the longitudinal velocities, u and w, the pitch rate, q and the angle of inclination, θ. In addition to the above states, the altitude h was augmented to get the full longitudinal dynamics model. The control input (δ_e, δ_t) is the elevator deflection angle δ_e , and the engine throttle lever δ_t.

8.7 Lateral Stability

$$\begin{pmatrix} \dot{\beta} \\ \dot{p} \\ \dot{r} \\ \dot{\varphi} \end{pmatrix} = \begin{pmatrix} -2.7807 & 0 & -1 & 0.4454 \\ -0.9829 & -37.2222 & 0.2987 & 0 \\ 1539 & -355.6234 & -75.4193 & 0 \\ 0 & 1 & 0 & 0 \end{pmatrix} \begin{pmatrix} \beta \\ p \\ r \\ \varphi \end{pmatrix}$$

$$+ \begin{pmatrix} 0 & 1.7536 \\ 272.3764 & 0.2987 \\ -410.2334 & -793.4244 \\ 0 & 0 \end{pmatrix} \begin{pmatrix} \delta_a \\ \delta_r \end{pmatrix}$$

Where β the sideslip angle, p and r is represent the roll and yaw rates and_ is the roll angle. The aileron controls input is denoted by δ_a, and the rudder control input δ_r.

9 Structures & Loads

9.1 V-N Diagram

In order to define the final configuration of WAAPI UAV, the applied loads during its operational life flight and ground conditions, need to be known. These three limits are shown in the load factor diagram, where every point represents the load condition of WAAPI UAV during maneuvering at the correspondent true airspeed (ft/s). Table 9-1 contains WAAPI UAV data necessary to build the load factor diagram. Within the bounds of the load factor diagram, one gets the safety flight conditions specified. The wind gusts are movements of ascending air, perpendicular to the ground, which change the incidence and the relative speed of the aircraft. Gust loads can be seen as an increase in the load factor; for this reason, it is necessary to define a new field of safety. The wind gust load and load factor diagrams shown in Figure 9–1.

Table 9-1 Airplane and flight conditions data required to define the V-n diagram

Parameter	Symbol	Value
Air Density (kg/m^3)	ρ	0.00237
Max take-off weight (N)	W_{to}	36
Max lift coefficient	$C_{L\ max}$	1.221
Min lift coefficient	$C_{L\ min}$	0.257
Lift curve slope (rad^{-1})	$C_{L\ \alpha}$	6.01
Wing span (ft)	b	10.39
Wing surface (ft^2)	S	9
Mean geometric chord (m)	c	0.866
Wing loading (lb/ft^2)	W/S	4

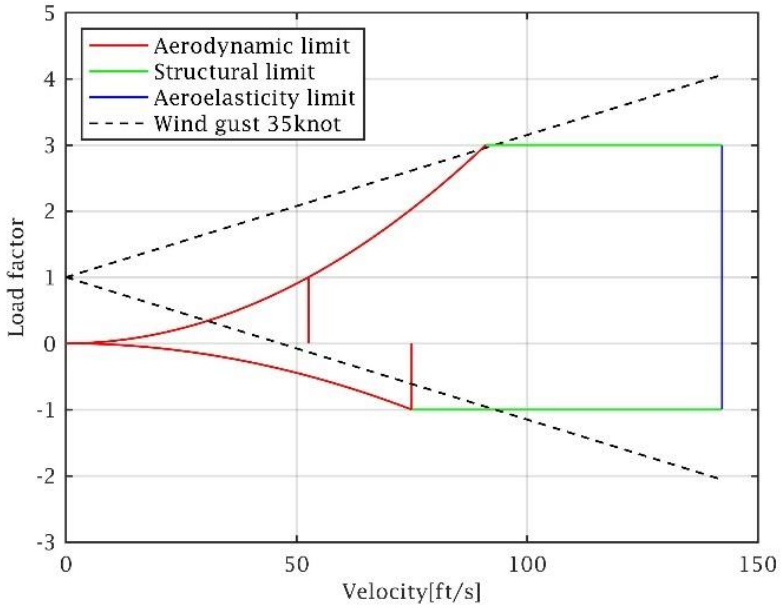

Figure 9–1 V-n diagram for maneuvering limits and gust loads.

The complete flight envelope diagram, also called V-n diagram, is built by superimposing the maneuvering diagram and the wind gust diagram, this diagram shows in Figure 9–2 is used to delineate the proper field in which the accordingly WAAPI UAV can fly to design the structure. The characteristic data emerging from this diagram is used for the next step of the load determination, is shown in Table 9-2.

Table 9-2 Characteristics data for WAAPI's flight envelope

Data	Velocity (m/s)	Load Factor
V_{st+}	52.49	1
V_{st-}	74.95	-1
V_A	91.08	2.96
V_C	91.86	2.99
V_D	142.29	3
V_G	59.07	-1

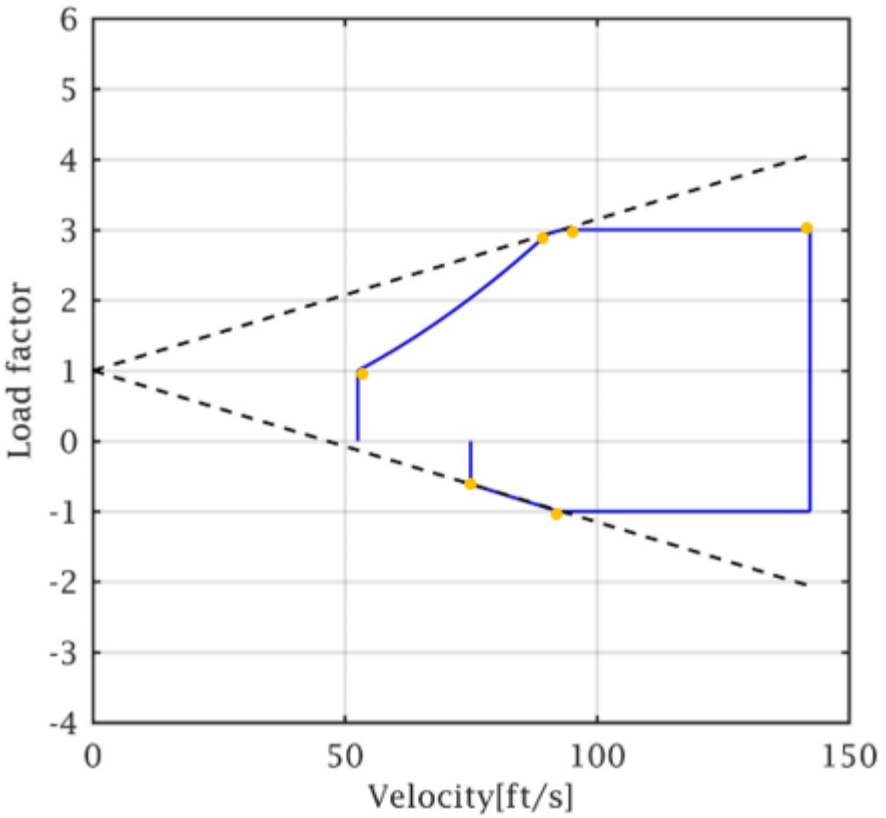

Figure 9–2 complete flight envelope for WAAPI

9.2 Unmanned Aircraft Loads

The gust and maneuver loads are obtained by developing V-n diagrams. A major output of the V-n diagram is the maximum positive and negative load factors that are used to estimate aerodynamic then size the structures. XFLR5 was used to simulate important data of the 3D wing. Distributed loads are calculated using the MTOW. [5]

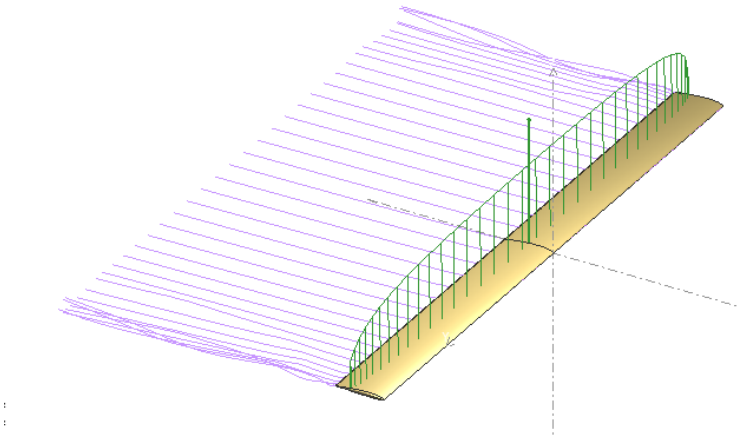

Figure 9–3: Aerodynamic analysis in XFLR5

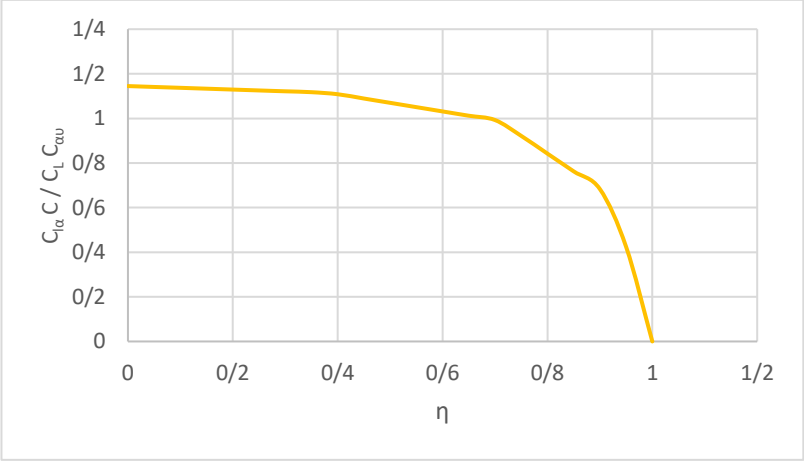

Figure 9–4 Spanwise additional lift distribution curve

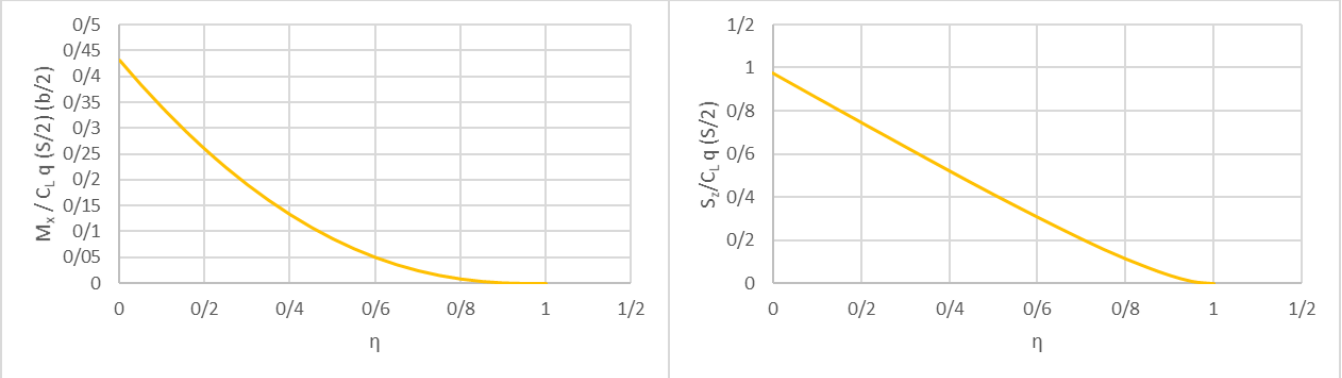

Figure 9–5 Left: Spanwise bending force distribution (resulted from additional lift) | Right: Spanwise Shear force distribution (resulted from additional lift)

To determine all forces on the wing, it is required to calculate inertia force distribution. To calculate this distribution Boom's weight and its effect on the wing will be considered.

Boom is described as a beam constrained in the spar (at the front) and loaded at end of the beam. The calculation is simplified only one boom loaded by half of total load to boom. The model and free body diagram for this case are shown as follows.

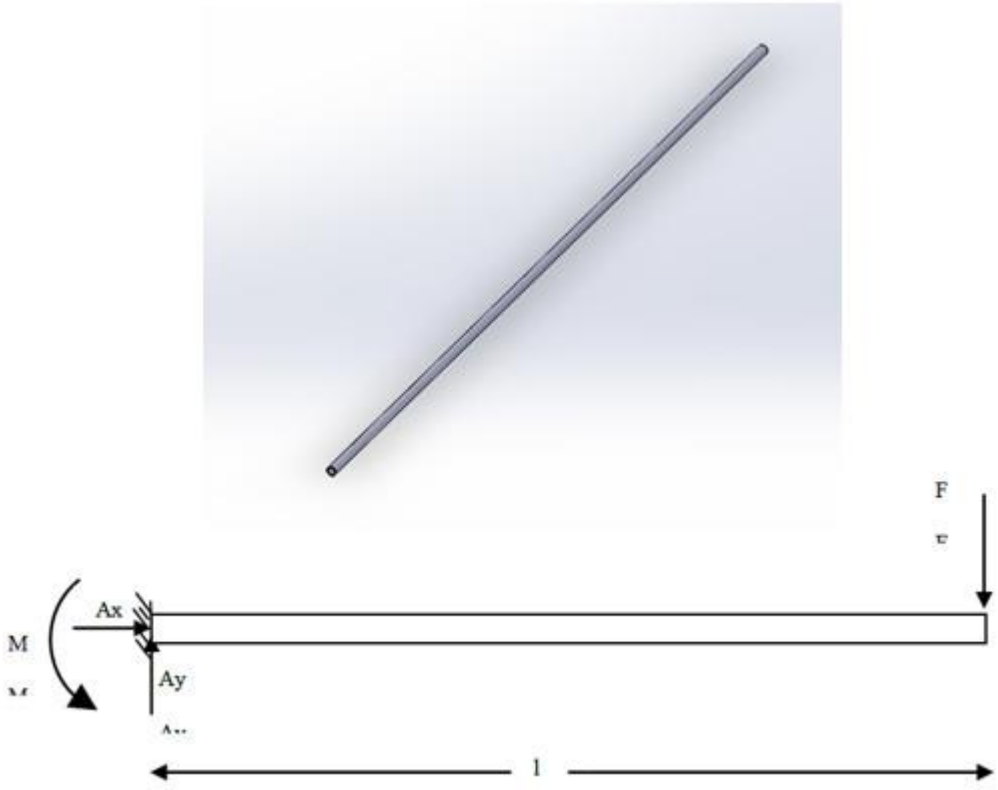

Figure 9–6 Boom and free body diagram

With assuming spanwise linear weight distribution of, wing inertia force diagrams can be found below:

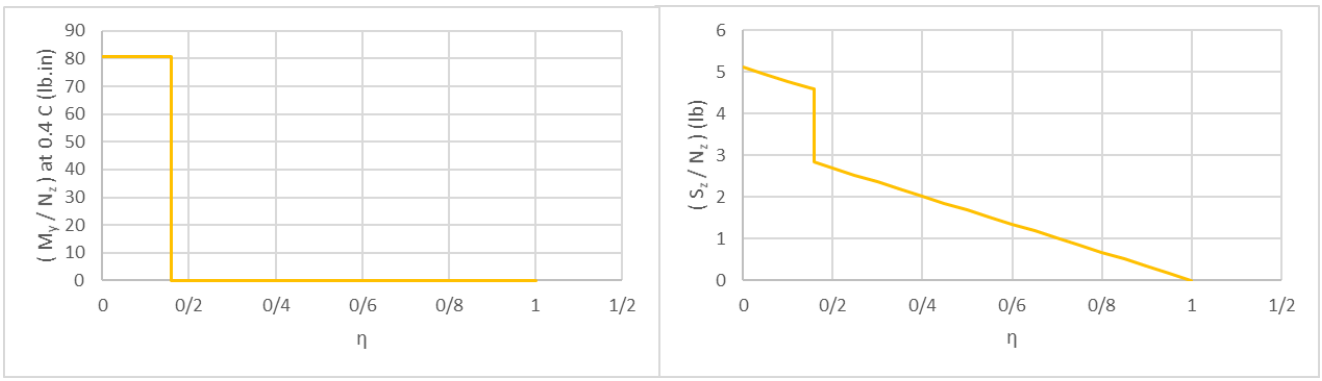

Figure 9–7 Left: Wing inertia | Right: Spanwise inertia force distribution

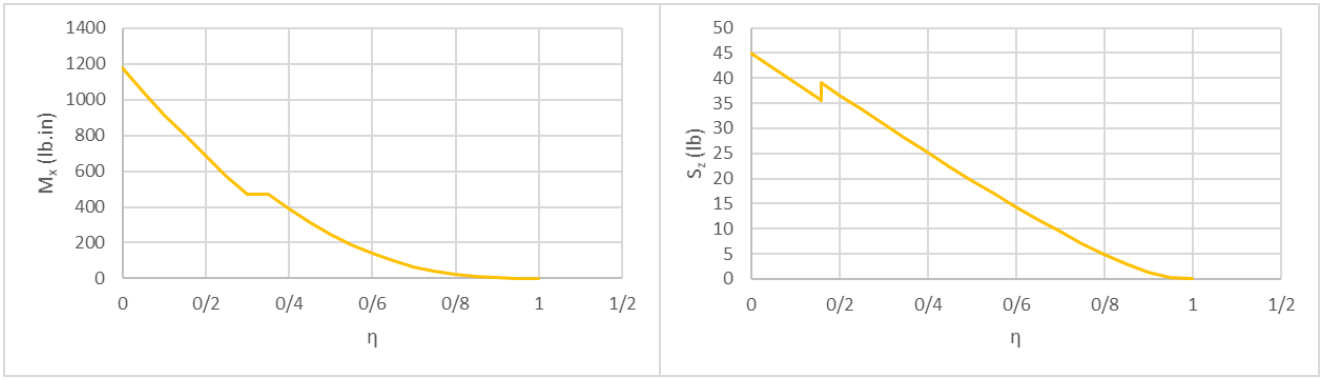

Figure 9–8 Left: Wing bending moment | Right: Wing shear load

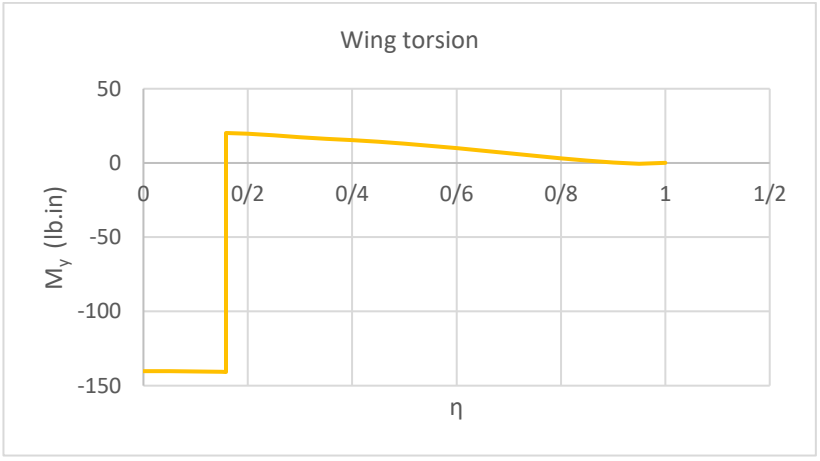

Figure 9–9 Wing torsion

9.3 Materials Selection

Some important factors have been considered during the selection of a material for WAAPI UAV. This material should have low density, high strength, high stiffness, reduced machining, corrosion resistance,

and vibration damping ability. Cost is also an important factor to choose material and manufacturing products should be done in a short time.

Metals and composite are examined for WAAPI structure material. Metals are ease of analysis, low cost, robust environmental characteristics (temperature, humidity, UV, abrasion), ease of maintenance, and good performance. But according to analysis, airframe weight will increase by 29% by using metals for the airframe. Also because of need to machining (in case of using metal), the rate of production will decrease and it will increase the unit cost of WAAPI. Designed aircraft's wing has no taper and it was planned to use 3D printing technology for some elements in UAV. Even though metal materials are low cost rather than composites, but investigating manufacturing cost for both group of materials results that metals need more manufacturing man-hour and less production rate and by using composites, some elements (like wing ribs) can be produced by using 3d printing technology and airframe weight will be less than a metal airframe and this additional weight results in more fuel consumption and higher operating cost.

Large manufacturing variations reduce the allowable properties used to size the structure, leading to additional materials to ensure that the structure is reliable and will decrease manufacturing cost.

9.3.1 Wing, Tail, and fuselage Material

The composites used in unmanned vehicles divided into two basic groups – metal matrix composites (MMCs) or polymer matrix composites (PMCs) – which are then reinforced with fibers or particles of another material that is typically more brittle but far stronger and stiffer than the matrix. The composite material is been chosen consist of two phases (fiber and matrix material) with significantly different properties. Polymer Selected as matrices materials because of several reasons. PMCs has given us excellent strength-to-weight properties and easier manufacturing than MMCs. numerous polymer matrix composites were studied. Fabric E glass is selected. Mechanical properties of polymer matrix composites are listed in Table 9-3.

Table 9-3 Mechanical properties of polymer matrix composites

	Symbol	Units	Std CF Fabric	E glass Fabric	Kevlar Fabric	Std CF UD	E glass UD	Kevlar UD
Young's module 0°	E1	GPa	70	25	30	135	40	75
Young's module 90°	E2	GPa	70	25	30	10	8	6
In-plane Shear Modules	G12	GPa	5	4	5	5	4	2
Major Poisson's Ratio	υ12		0.1	0.2	0.2	0.3	0.25	0.34
Ult. Tensile Strength 0°	Xt	MPa	600	440	480	1500	1000	1300
Ult. Comp. Strength 0°	Xc	MPa	570	425	190	1200	600	280
Ult. Tensile Strength 90°	Yt	MPa	600	440	480	50	30	30
Ult. Comp. Strength 90°	Yc	MPa	570	425	190	250	110	140
Ult. In-plane Shear Strength	S	MPa	90	40	50	70	40	60
Density		Kg/m^3	1600	1900	1400	1600	1900	1400

9.3.1.1 Wing Spar Material

A high strength, some flexibility, lightweight material has been chosen to the wing spar, considering the aerodynamic loads, and the cross-section geometry selected in Table 9-5 shows the comparison between an aerospace isotropic aluminum alloy, 7075-T7451 [6], with three polymer matrix composite materials. CFRP has the largest ratio, besides, it has almost the same Young's Modulus of the aluminum alloy. Nevertheless, CFRP is very expensive and time-consuming to make CFRP selected to compose the WAAPI Spar. To prevent the laminate from bucking, high-density foam is used as a core. It also facilitates the manufacturing process, because the laminate can be laid-up directly on the core. Divinycell H45 foam is chosen due to its machinability, mechanical properties, and low weight. Table 9-4 shows its main mechanical properties.

Table 9-4 Mechanical properties of Divinycell H35

Divinycell H 45		
Property	**Unit**	**Value**
Nominal density	lb/ft^3	3.0
Compressive strength	Psi	87
Compressive modulus	Psi	7250
Tensile strength	Psi	203
Tensile modulus	Psi	7975
Shear strength	Psi	81
Shear modulus	Psi	2175
Shear strain	%	12

9.4 Wing Cross Section Design

9.4.1 Spar Cross Section

The lift distribution along the wingspan is the most relevant load causing a large bending moment on the spar. To design an efficient spar, the cross-section should be chosen carefully, to maximize its moment of inertia.

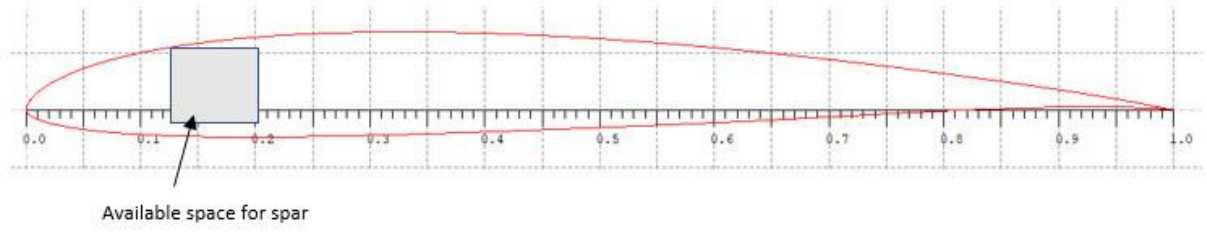

Figure 9–10 Wing rib

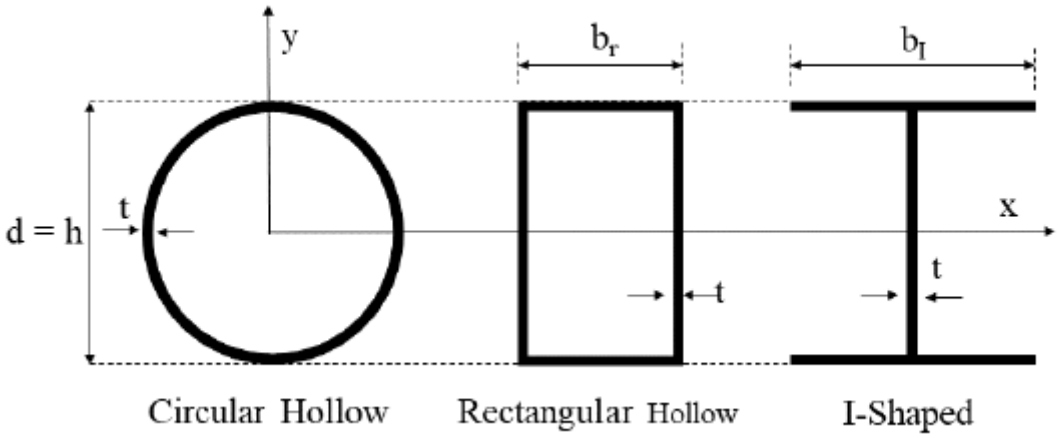

Figure 9–11 Cross-section comparison

Table 9-5 Cross section comparison

	Symbol	Circular	Rectangular	I-shaped
Torsion Constant	K	3.9009	2/2423	0/0022
Moment of Inertia	I_{xx}	1/0928	3/6	3/24

Table 9-5 shows that the circular hollow cross-section is better to withstand twisting moments, because of its higher torsion constant. However, the rectangular thin-wall cross-section has a higher moment of inertia along the X-direction, almost 12 times larger than the circular section. Considering that the spar should resist bending moments rather than torsion moments, the rectangular thin-wall cross-section is chosen.

9.4.2 Boom Cross Section and material

Boom material and its specification is selected off-the-shelf, this decision will reduce RDT&E cost. Selected boom material and cross section dimensions is listed in Table 9-6. [7]

Table 9-6 Boom material and cross section dimensions

Material	Inner radius (in.)	Outer radius (in.)
Carbon fiber	0.57	0.63

9.5 Landing Gear

To perform the landing in concrete, wood, asphalt, hard turf, and grass field; a landing gear must be designed, because During landing, it acts as shock absorbent mechanical structure to absorb and transmit a majority of impact energy is dissipated and this event make aircraft structure's resistance to damage during life-cycle and reduce its life-cycle cost, because boom's material is carbon fiber and WAAPI has a composite propeller and also if Gimbal's actuator doesn't work properly (being mal-function) it will damage EO/IR cameras.

The Tricycle-type, shown in Figure 9–12, was selected for the aircraft. This configuration allows the aircraft to brake faster without the aircraft nosing over. This also, evenly distributed weight of aircraft increases stability and ensures safety as well as cross wind Cross winds do not affect the aircraft. The landing gear was sized using the method outlined in Roskam. [1] Tricycle landing gear geometry is listed in Table 9-7.

Table 9-7 Tricycle landing gear geometry

track	**2.31ft**
wheelbase	2.66ft
φ	44°

Figure 9–12 Tricycle landing gear geometry

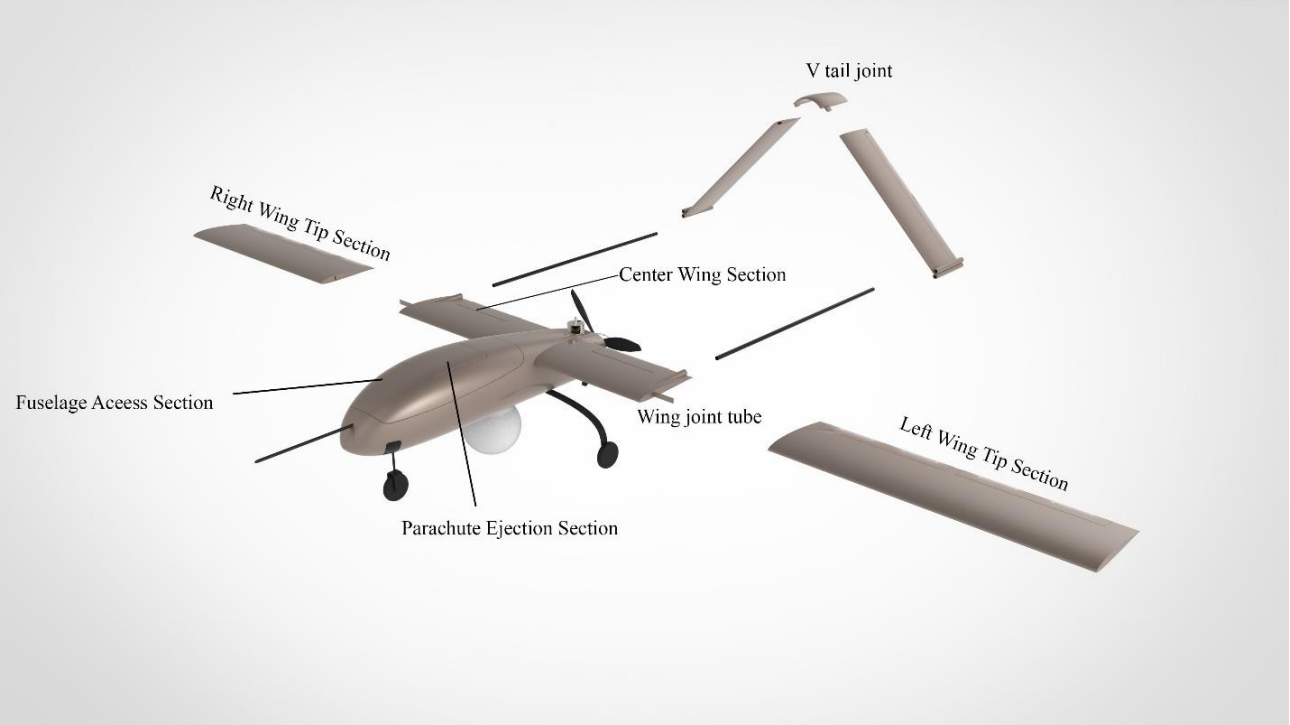

Figure 9–13 Structure exploded view

10 Weight & Balance

10.1 Major Component Weights & Locations

The needed components which WAPPI carries are determined and the weight and dimensions are calculated. Aircraft structural weights were determined by Preliminary and Detail Design Mass Properties Methods. [4] For fiberglass composite material structural weight estimation, the number 1 factor is used.

Propulsion system weights were determined according to the information presented on their website [9] and the database of propulsion components. [10]

All the avionics, batteries and subsystems needed for the aircraft is determined and the dimensions, weight and the required power are obtained. Also weight of the generator which fulfil the mission required power is calculated. This information is defined in the Avionic part.

For the emergency situations one parachute is carried in the fuselage and its weight is calculated in the recovery part.

The summation of all of the weights & balances work for the WAAPI UAV can be found in Table 10-1.

Table 10-1 Empty center of gravity calculation

weight and balance	Weight (lb.)	$X_{C.G.}$ (in)	$Y_{C.G.}$ (in)	$Z_{C.G.}$ (in)
pitot tube	0.12	0.78	0.00	10.56
RIEGL miniVUX-1UAV	4.4	4.78	0.00	10.04
parachute	0.77	14.49	0.00	6.57
avionic	0.77	14.49	0.00	8.66
back up battery	1.39	14.49	0.00	11.36
gimbal	5.00	22.75	0.00	3.35
camera1	0.15	22.75	0.00	3.35
camera2	0.38	22.75	0.00	3.35
ECU	0.18	22.75	0.00	7.68
Generator controller	0.44	22.75	0.00	6.99
fuel tank	0.13	28.56	0.00	9.09
fuel	2.25	28.56	0.00	9.09
Propulsion System	5.25	36.7	0.00	10.24
right wing	3.37	30.00	31.17	14.96
left wing	3.37	30.00	-31.17	14.96
fuselage	3.30	17.71	0.00	10.43
right boom	0.64	53.90	3.94	14.96
left boom	0.64	53.90	-3.94	14.96
tail	2.20	75.01	0.00	24.80
nose gear	0.45	7.09	0.00	3.35
main gear	0.93	31.89	0.00	3.35

Table 10-2 WAAPI center of gravity location

$X_{C.G.}$ (in)	$Y_{C.G.}$ (in)	$Z_{C.G.}$ (in)
10.65	0.00	27.44

10.2 Center of Gravity Envelope

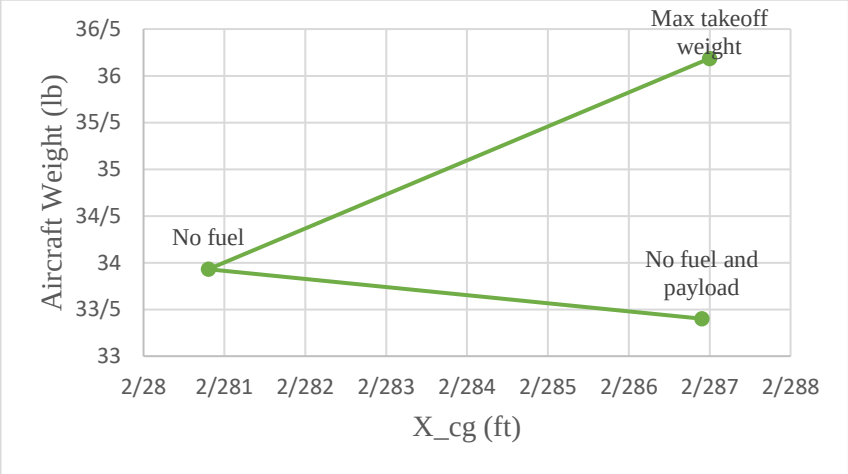

Figure 10–1 Center of Gravity Excursion Diagram (with EO/IR camera)

Table 10-3 Static margin shift (with EO/IR camera)

Static margin shift	
At takeoff gross weight	8.91%
At empty weight + payload (no fuel)	9.60%
At empty weight (no payload, zero fuel)	8.90%

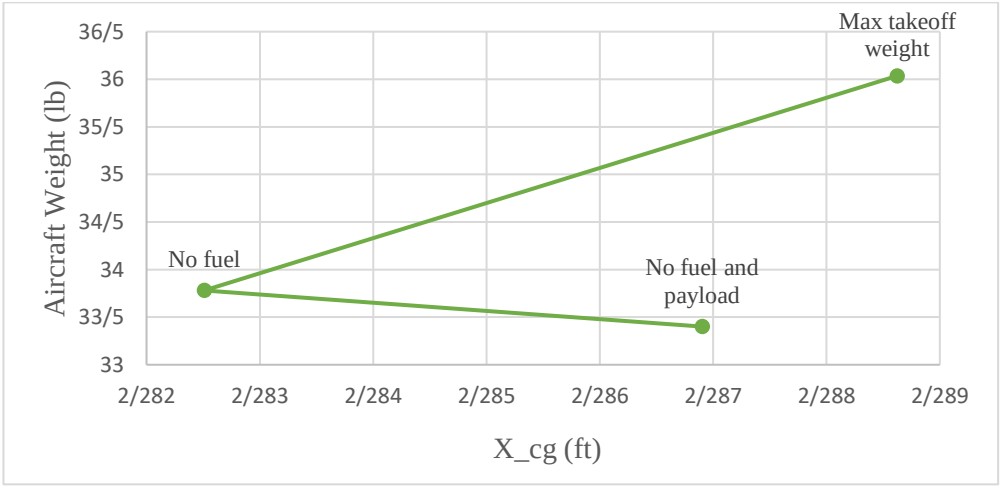

Figure 10–2 Center of Gravity Excursion Diagram (without IR camera)

Table 10-4 Static margin shift (without IR camera)

Static margin shift	
At takeoff gross weight	8.91%
At empty weight + payload (no fuel)	9.41%

At empty weight (no payload, zero fuel)	8.71%

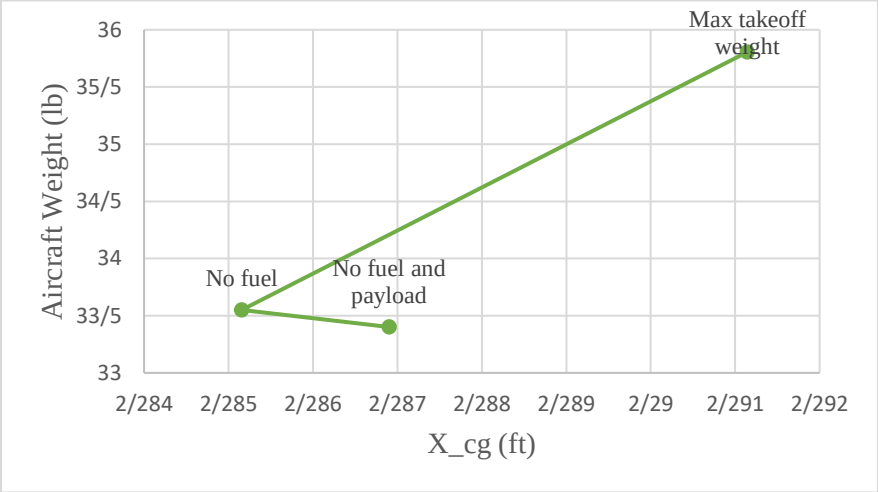

Figure 10–3 Center of Gravity Excursion Diagram (without EO camera)

Table 10-5 Static margin shift (without EO camera)

Static margin shift	
At takeoff gross weight	8.91%
At empty weight + payload (no fuel)	9.11%
At empty weight (no payload, zero fuel)	8.43%

Figure 10–1, Figure 10–2, and Figure 10–3 and also, Table 10-3, Table 10-4, and Table 10-5 shows that the WAAPI remains stable.

11 Propulsion Systems

The initial horsepower requirement of the engine has been determined in Figure 4–2 and propulsion system can be selected based on the constraint analysis section.

There are two choices for the energy source of WAAPI, Electrical based or fuel based. Electric motors have multiple advantages. Unlike internal combustion engines, there is very little maintenance and no consumables such as liquid fuel and lubricants. Electric motors can be stored for very long periods of time. The biggest limitation of electric flight is the short endurance that can result from the power source. Namely, modern batteries have low specific energy relative to liquid hydrocarbon fuel, resulting in UAs with only

0.5 to 3 hours of endurance another disadvantage is most operational electric aircraft are small, usually weighing less than 20 lb. and using motors with less than 1 kW. And electric motors need batteries to provide their energy and using batteries will highly increase the operating cost (cost of purchasing a typical lithium-ion battery is 200 USD/kwh)

11.1 Engine

Reciprocating engines are the most common form of propulsion for UAs with takeoff gross weight values between 20 and 2,500 lb. Commercial-off-the-shelf (COTS) engines are widely available between1–200 hp. Reciprocating engines come in many forms. The most prevalent are two-stroke, four-stroke, and rotary engines. We chose Two-stroke glow fuel engine witch it requires a fuel-oil mixture. The high power-to-weight ratio, less engine vibration, and low cost are the most important considerations. The initial horsepower requirement of the engine, 3.1 brake horsepower this value was then taken to UAV database to find off-the-shelf engines that met the power requirement. 18 engines have been checked and among them, 4 engines have been selected to compare, this selection has been made base on the power required for the mission. A list of specifications of comparable Reciprocating engines is shown in Table 11-1.

Table 11-1: two-stroke / four-stroke /Gasoline Engine weights & maximum power output

Engine	Manufacturer	Max Power	P/W ratio	Cost	Time Between Overhaul
3W-28i CS	3W Modellmotoren	3.6 Hp	1.35	900 USD	1200 hours
120AX	O.S. Engines	3.1 Hp	1.62	300 USD	250 hours
GT33	O.S. Engines	3.8 Hp	1.77	450 USD	250 hours
DLE-55RA	DLE	4.1 Hp	1.64	350 USD	Not found

Despite less power to weight ratio for 3W-28i CS, this engine has more time between overhaul and this specification results in less operating cost for engine replacement and lower life-cycle cost.

3W-28i CS was chosen for its size, weight, specific fuel consumption and brake horsepower. The enormous power development makes it comparable to other engines with larger displacements. The 3W

Competition series (CS version) distinguishes itself through greater performance, more rapid response behavior, and high torque. The engine thereby achieves a high standard of performance. Transfer ports in the cylinder and crankcase are modified. Reciprocating engine thermal efficiency is typically 15% and η_m is the mechanical efficiency, which accounts for friction, power for generators and other losses .High humidity combined with high temperatures can produce up to a 20% reduction in available power. [9]

Table 11-2: two-stroke / four-stroke /Gasoline Engine weights & maximum power output

Engine Configuration	
Engine Manufacturer	3W Modellmotoren
Model	3W-28i CS
Max Power	3.6 Hp
SFC	750 ccm/hour
Dry Weight	1.210 kg
P/W ratio	1.35
Displacement	28.5 ccm

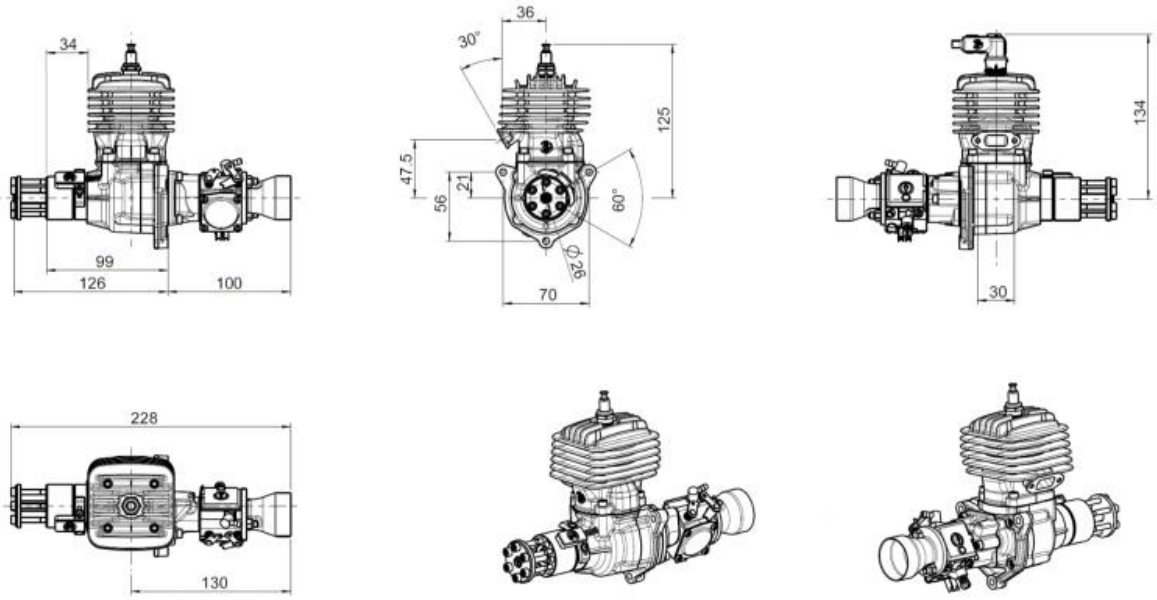

Figure 11–1: Views of Engine

11.2 Propeller Selection

Propeller selection for aircraft has been done according to a number of factors: manufacturer recommendations, engine type, power RPM range, cruise speed, noise abatement issues, and type of aircraft are limited to a rather short propeller due to the pusher design. Other factors include composites, wooden or metal type propellers. Composite propellers dampen the engine vibration much better which may lead to reduced blade failures. After checking propellers that meet WAAPI's requirements, the suggested company's propeller (with Carbon Fiber-Enhanced Plastics material) has been selected and this selection (Of the Shelf) will reduce RDT&E cost. The propeller's specifications are shown in Table 11-3.

Table 11-3: Propeller Specification

Propeller Parameter	Values at Cruise Conditions
Number of Blades	3
Diameter	17 in
Nominal pitch	10 deg

Frontal Propeller Area	227 in^2
Tip Mach number	.13

Instead of designing an inlet for WAAPI, Engine's fins located (is shown in Figure 11–2) out of fuselage to reduce fuselage's diameter and manufacturing cost and avoiding high temperature in the fuselage.

Figure 11–2 Engine Fins

11.3 Muffler

Mufflers reduce the acoustic signature of the engine. The volume of effective mufflers has a significant impact on the UA design and we considered at the earliest stages to ensure that the fuselage is sized appropriately. We selected mufflers have been specially matched and developed for our engine. They lend the engine good performance and very good running behavior in the mid-rotational-speed range. Noise development is minimized. We select the matching muffler size based on the displacement of the engine used to give the WAAPI, the ability of engine replacement (with other types).

Table 11-4: Muffler Specification

Parameter	Value
Diameter	2.16”
Length	12.2 in
Max. cylinder capacity	1.83 in^3
Mussel manifold length	6.7-7.48 in
Weight	0.38 lb.
Connection tube diameter	0.08 in

11.4 Engine Performance Analysis

The performance of a two-stroke engine was evaluated and modeled using a single shot combustion Experiment. The following process used to estimate the integrated engine propeller performance [3]:

The total shaft power required is the sum of P_{Shaft_Prob} and the generator load:

$$\text{Equation 11-1 } P_{Shaf} = P_{Shaft\_Prob} + \frac{P_{Gen}}{\eta_{Gen}}$$

Generator power has been determined by calculating avionics required power.

Fuel flow rate was calculated by the Equation 11-2 [3]:

$$\text{Equation 11-2 } \dot{m_{Fuel}} = BSFC.P_{Shaft}$$

I contact with 3W Company and ask them to provide me the SFC of the engine and they accept to provide me that information.

Results of engine performance analysis is shown in Table 11-5.

Table 11-5: Engine Performance Analysis

P_{shaft_prop}	P_{shaft}	P_{Gen}	η_{Gen}	BSFC
3.1	3.3	.15	0.85	0.57

11.5 Fuel System

Fuel system includes tank 0.148 $ft^3$and fuel filter. Fuel filters improve performance, as the fewer contaminants present in the fuel, the more efficiently it can be burnt. The tank involves a very rugged version of a round, fuel-resistant clunk tank. The large opening makes possible easy installation of the built-in tank components. Used fuel for the engine (3W-28i CS) is fueled with octane 92+, and also heavy fuels (JP-5 or JP-8) has been used with this engine. in fact, Heavy fuel is less volatile than pump gas or glow fuel, thereby improving handling safety. But these fuels are more expensive and will increase operating cost.

12 Avionics, Flight Software, and Subsystems

12.1 Avionics

Avionics systems applied into WAAPI were adapted from standard aviation avionics. The avionics components includes navigation sensors, Air Data Systems, Engine Controller, Airspace Integration System, Autopilot, UA Management Systems, and Mission Management Systems.. Avionics size, weight, and power have been fully accounted for the mission. Specification of components listed in Table 12-1.

12.1.1 Navigation Sensors

The VN-100 is a miniature, high-performance Inertial Navigation System (INS) that combines MEMS inertial sensors, and advanced Kalman filtering algorithms to provide optimal estimates of position, velocity, and attitude.

12.1.2 Air Data Systems

UAV Factory's heated Pitot-static tube is fully integrated into the tube which allows for minimal power consumption. An onboard feedback controller continuously regulates the temperature of the probe and automatically switches off the heating element when the required temperature is reached.

12.1.3 Engine Controller

EcoTrons ECU added to engine system to improve reliability and fuel consumption. Engine control algorithms implemented in the ECU are based on the very mature Aaronic SM4 platform. This platform uses a patented control strategy specifically targeted for use on multi-throttled and low-manifold vacuum engines, with the excellent performance achieved for two-stroke engines. ECU provides a complete single-supply solution, with integrated high-power injector and ignition drivers, servo control of throttle position, closed-loop fuel pump control and a 6V supply for use with throttle servos and ignition units.

12.1.4 Recovery System

Marco Polo is simple to set up and use, single button-push to begin searching for lost UAV with real-time Distance and direction feedback Works anywhere, totally self-contained, no GPS or cell network required, no monthly service contracts, ideal for remote areas Rechargeable lithium-ion battery in transceiver tag gives us up to 15 days to find our lost UAV.

12.1.5 Autopilot

A number of autopilots such as "MicroPilot MP2128g", "CloudCap Technologies Picolo", "Kestrel", and "Pixhawk 4", the RFP emphasizes on being low cost and between mentioned options, "Pixhawk 4" has the least price and will meet operation's requirements. So "Pixhawk 4" has been selected to use in the WAAPI.

The Pixhawk 4 is equipped with new sensors with higher temperature stability, integrated vibrations isolation, increased ease-of-use: pre-installed with most recent PX4 (v1.7), and extra ports for better integration and expansion. It contains the most advanced processor technology from ST Microelectronics,

sensor technology from Bosch, Intenseness and a Nott real-time operating system, delivering incredible performance, flexibility, and reliability for controlling any autonomous vehicle. More complex algorithms and models can be implemented on the autopilot.

12.1.6 Computers and Processors

The flight control computer is an FPGA based embedded processing system our objective for selecting FPGA is lightweight, small and have adequate processing power at low power consumption to maintain long flight times

Table 12-1: Avionics components of UAV

Name	**Type**	**Size (in)**	**Weight (lbs)**	**Power (W)**	**Cost (USD)**
VN-100	IMU	1.41*1.3*0.55	0.033	0.48	1300
Marco Polo	Locator	2*1.375*0.75	0.0625	0.00	235
Heated Pitot-Static Probe	Pitot Tube	9.4	0.125	19.2	435
Pixhawk 4	Autopilot	1.73*3.3*0.47	0.0348		220
EcoTrons ECU	ECU	2.52*3.09*0.78	0.264	8.64	600
Ping 2020i	ADSB transceiver + GPS	0.98*1.57*0.63	0.050	0.5	1400

12.2 Sub-Systems

WAAPI payloads, communications systems, and avionics consume power. The required power is generated by generators. In case of engine or generators problem back up battery would be used. The generator system specification is shown in Table 12-2.

Table 12-2 Generator system electrical specification

Generator voltage range	10-35 V
External power supply voltage range	13-50 V
Battery type	3 cells, Lithium Polymer
Battery voltage	12.6 V
Maximum battery charging current	2 A
Maximum continuous generator current	4.3 A

Maximum continuous battery current	8 A
Maximum continuous external power current	8 A
Output voltage	6 V and 12 V
Maximum output voltage ripple	50 mV @ 6 V, 50 mV @ 12 V
Continuous load current, 6 volt output	5 A

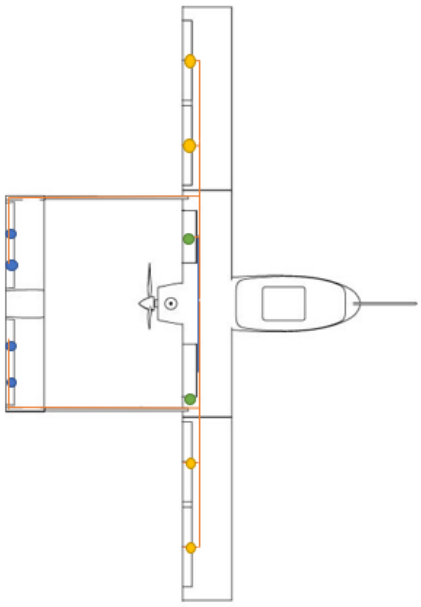

Figure 12–1 WAAPI control surfraces's actuators

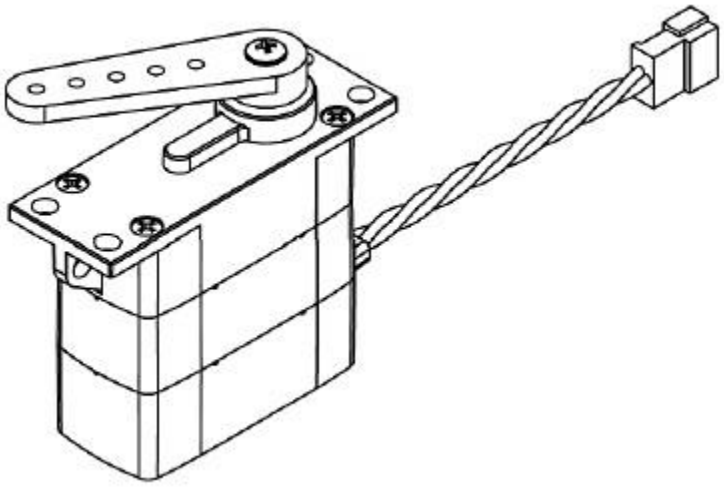

Figure 12–2 DA-14 actuator

13 Launch and Recovery

13.1 Ground-Vehicle Launch

13.1.1 Car Top Launch

WAAPI can be launched from moving pickup truck. The pickup truck provides the acceleration to takeoff speed (63fps), when takeoff speed is reached, Autopilot performs a pull-up maneuver to allow the aircraft to separate from the pickup truck.

To decreasing the RDT&E cost, used launcher will be selected off-the-shelf, some factors has been considered to select the launcher, such as cost, weight, and reliability. In result of this consideration, UAV factory car top launcher has been selected for operation. The picture of the system is shown in Figure 13–1.

The car-top launcher has a convenient removable starter assembly with an integrated Lithium Ion battery and MOSFET switch. Once the UAV engine is running, the starter assembly can be easily removed.

Some advantages of car top launching are:

- Low cost alternative to catapult launching
- Light, small and reliable
- Good reliability under strong wind, side wind and gusty conditions
- Safe and reliable electric starter with Lithium batteries, MOSFET switch

Figure 13–1 Car Top Launch System

13.2 Parachute Recovery

To ensure the safety of aircraft and its payload, it is needed to use an emergency recovery system to recover the vehicle safely. It is also can be used to recover UAV in case of lack of existence a safe area for landing. There are some methods to recover aircraft safely, some of these methods are:

1. Belly landing

This method has been used in some UAVs like EWG-E2/E3 UAV, Altavian NOVA F7200, and Aeromapper 300, this UAVs has MTOW below 25 lbs. and this recovery method can damage aircraft avionics and its payload.

2. Parachute

This method is very common in SUAS class and some of its advantages are low descent rate and little horizontal speed. And among its disadvantages can mention that this method needs an additional airborne system.

3. Net Recovery

This method needs a system mounted on a truck that increases cost and its more important disadvantage is that this method doesn't ensure the safety of aircraft and its payload. (Cause of quick deceleration)

4. Water Recovery

This method requires special geographic location but it will be a suitable option in case of access to lakes.

5. Deep Stall

This method used for UAVs that weigh less than 20 lbs. and can't ensure the safety of aircraft and its payload.

In the result of the above discussions, using a parachute for emergency recovery of WAAPI considered in design and sizing of the parachute will be done in the following sections.

13.2.1 Parachute Sizing

Table 13-1 Results of parachute sizing

Purpose	**Chute Size (ft^2)**	**Mass (lbs.)**	**Rate of Descent (ft/s)**	**C_D**
Landing and Emergency	55.2	1.54	16.4	2

13.2.2 Deployment System

Generally, there are two methods to deploy a parachute

- **Passive Deployment** used to eject the parachute into the air stream for these system the chute is packed into a deployment bag. To help pull this from the compartment a small pilot parachute is

provided that will be easily caught by the wind and pull out the deployment bag. The harness extends until the bag is pulled off the chute.

- **Ballistic Parachute Deployment:** Also called active deployment the parachute is packed into some sort of container or canister. The various methods can be used to forcefully eject the parachute into the air stream. [11]

Passive deployment is a common method for fixed-wing UAVs and its cost is lower than ballistic deployment (both Unit cost and Operational Cost) and it has less weight (ballistic method requires a spring or a gas to deploy) and base on mentioned reasons it is reasonable to select and size a parachute with passive deployment ability.

14 Ground Control Station & Communication System

14.1 GCS Selection

In this section, a Ground Control Station (GCS) system will be chosen by consideration of:

1. Type of Operation
2. Ground Station will use the right front seat of 2018 Ford F-150 SuperCrew Cab
3. Ground Station will use 12V truck power
4. The communication antennas will be mounted to the truck.

14.1.1 SHELL Interface Model

Based on the operation and RFP understanding, a beyond line-of-sight GCS is required for UAS. SHELL interface model will be used to select GCS's components.

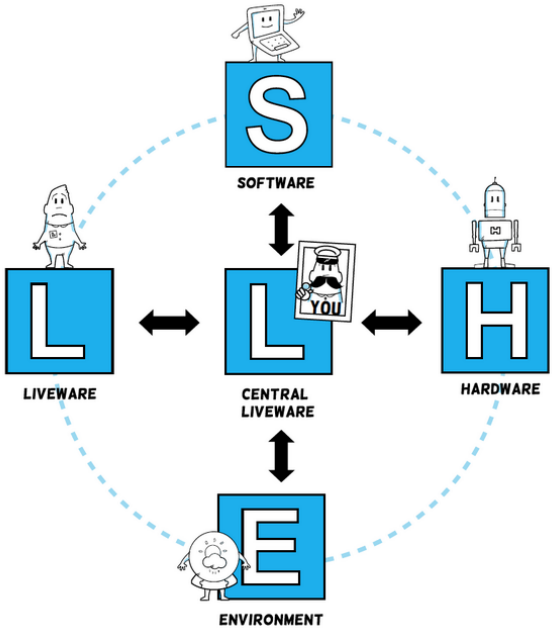

Figure 14–1: Shell Interface Model

14.1.2 Environment

Based on published RFP a “2018 Ford F-150 SuperCrew cab” is environment interface of GCS, this environment include vehicle’s cabin (for controller and GCSD4’s Suitcase) and bed (for GCS’s antenna) 2018 Ford F-150 cabin has 40.8” of Headroom and 43.9” of Legroom and its cabin volume 131.8 cu. Ft. Headroom and Legroom defined in Figure 14–2.

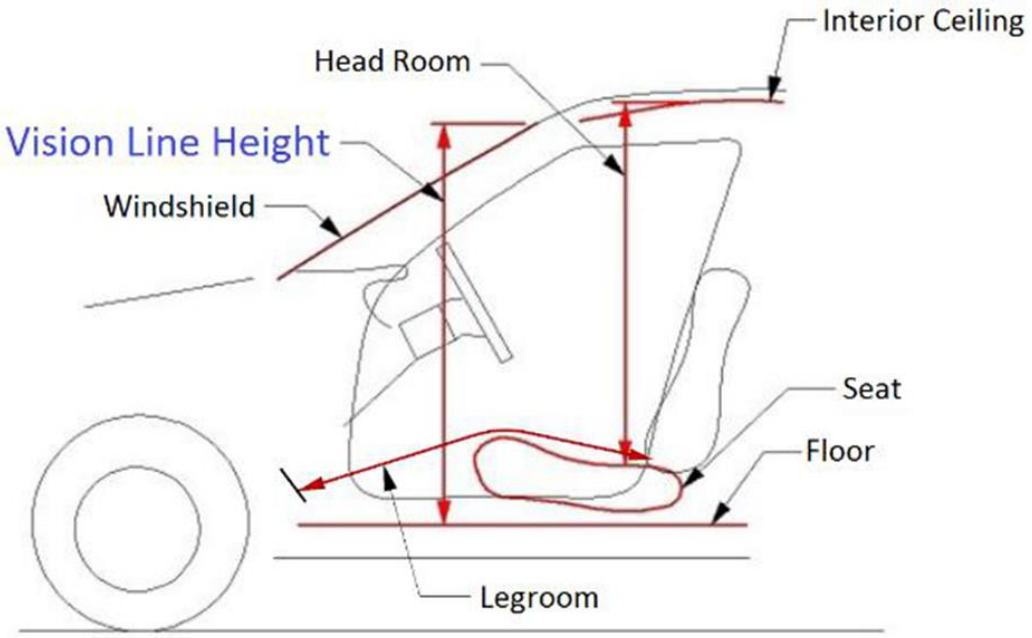

Figure 14–2: Headroom and Legroom Definition

14.1.3 Software

GCS's Operating System is Microsoft Windows 10© and its package include these software:

- DMDStudio (configuration and utility software for all XLRS systems in Windows environment)
- Mission Planner (It can be used to configure or control the autopilot, maps, and routes with Mavlink protocol)

Figure 14–3 Right: Mission Planner Software | Left DMD Studio Software

- Aerosim

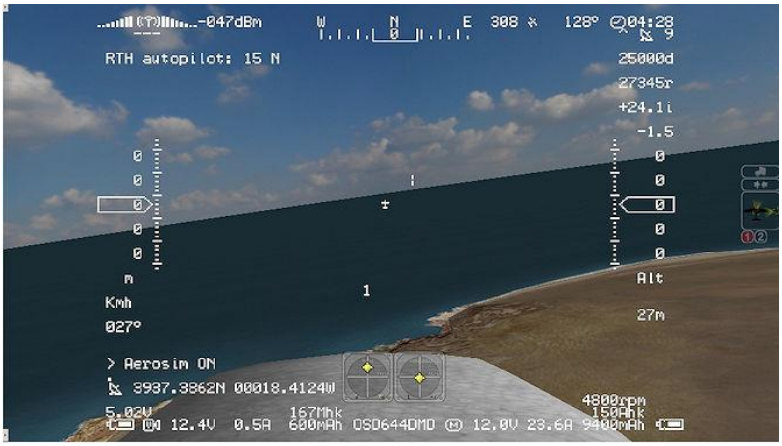

Figure 14–4: Aerosim Software

14.1.4 Hardware

Base hardware for UAS's ground station is a 2018 Ford f-150 SuperCrew cab and it is equipped with an XLRS product (GCSD4) that equipped with an RC and telemetry antenna (With the range of 108 nm) and analog video receiver and transponder (With the range of 43-54 nm). Embedded PC can be charged with 12-volt truck power, also its battery can provide power for its systems for 2.5 to 3 hours.

GCSD4 component is:

- RC Control:
- Safety Switch

With protective cover to not activate or deactivate it inadvertently

Figure 14–5 GCSD4 | Left: RC control view | Right: Safety control switch

- Embedded PC

With 7” touchscreen display

- FPV Video Screen

With 10” display

Figure 14–6 GCSD4 | Left: Embedded PC | Right: FPV Video Screen

- Suitcase

Robust, dustproof, water resistant (IP67 certified) and its temperature controlled by fans.

- Battery (Li Po)

Figure 14–7 GCSD4 | Left: Suitcase | Right: Battery

- Antenna planar and RXVID2-1C (Ground Antenna)

Figure 14–8 GCSD4 | Left: Antenna Planar | Right: Antenna (Ground)[1]

[1] Antenna planar in designed system is different from this picture

- ANTGSM24, XOSDV2, RXLRS. Professional RX, and ANTGSM900 (Airborne Systems)

Figure 14–9 GCSD4 | Left: XVID3 Analog Video System | Right: Professional radio control receiver

The integrity of mentioned hardware with autopilot (Pixhawk 4) has been checked and they have full compatibility with autopilot.

15 Payload System

Different payloads are required for the different missions designed for inspection of electrical power transmission, pipelines, roads, and railways. These payloads were created based on the concept of operations described above and the different customer attributes requested. Lays out exactly what pieces of equipment are compiled to make up the payload

15.1 High Resolution Camera

According to RFP and its requirements, a high resolution camera can be used to help identify specific tree species and identify transmission tower components that require repairs. Two types of sensors usually used for high resolution cameras:

- CMOS: Their cost and size is lower than CCD sensors, but provide a picture with higher noise, rather than CCD sensors.
- CCD: presented better pictures with less noise but their cost and energy consumption is higher.

CCD sensors have been selected because of less noise and better pictures with the cost of money and energy. Lumenera LT965R is selected to use with WAAPI UAV. This sensor provide us a 4k video during flight. This level of video quality will help the system to its mission (determine specific tree species and identify transmission tower components that require repairs) very well.

Figure 15–1 Lumenera LT965R (High resolution camera)

15.2 IR Camera

According to RFP, an IR camera will be used to determine the power line's temperature, with considering cost of the system, a FLIR Vue 336 9mm has been selected for the mission. This camera is a low cost solution and can provide us sufficient quality for our requirements.

Figure 15–2 FLIR Vue 336 9mm

16 Maintenance

In respect to the modular design of the WAAPI, the sections can be separated to be able to carry by the truck. Two boxes with defined dimensions are chosen for maintaining the sections; one contains the Wing tip sections, booms and tail sections, and the other contains the fuselage and the center wing sections which would be connected to the fuselage.

If the operator wants to carry non-essential out of WAAPI system components, one option is considered if no enough space is found, that is the car top launch that installed on the roof of the truck. The stall speed of the WAAPI is 52 ft/s thus not all the wing sections will be used in this case because of the stall speed.

According to [11], there is some factors in UAV maintenance that should be considered:

- Packing and transport: Small UAVs are generally disassembled between flights for transport and storage. A particular concern is the frequent connection and disconnection of electrical systems, which can increase chances of damage and maintenance errors. One advantage of UAVs compared to conventional aircraft is that they are not generally stored outdoors where they would be exposed to threats from the elements.
- Battery maintenance requirements: Batteries were noted as the cause of a high proportion of mishaps, both with the airborne and ground-based systems. Careful attention needs to be

directed to battery charging/discharging cycles. In addition, some types of batteries (e.g., lithium polymer) can be dangerous if correct procedures are not followed.

- Composite materials: UAVs tend to make extensive use of composite materials. Repair of these materials may require special expertise and equipment to deal with hazardous materials.
- Repair work by UAV manufacturer: The small size of many components and the modular approach to many UAV designs enables operators to ship damaged components back to the manufacturer for repair. A trend was detected indicating that minor maintenance was performed by operators, but major repairs generally involved sending the UAV back to the manufacturer.
- Recording of flight hours: UAVs do not generally have on-board meters that record airframe or engine flight hours. If this flight history information is not recorded by the ground station, the timing of hours flown must be recorded manually for maintenance purposes and inspection scheduling. But WAAPI UAV and its autopilot (Pixhawk 4) equipped to a flight data recorder and has ability to provide required information.

Engine maintenance: according to [9] after every mission, engine requires following maintenance and inspection:

- Check the spark plug for electrode cleanliness.
- The electrode gap must be 0.4 mm.
- Clean the air filter regularly.
- Check the muffler for possible oil-carbon deposits.
- Check the manifold for possible oil-carbon deposits

17 Cost Analysis

17.1 Aircraft Cost Estimation

In this section Gundlach and Roskam [1] methods and gathered data will be used to calculate RDT&E, manufacturing, and operation cost of the aerial vehicle.

In Roskam method cost of avionics, Instruments, and engines directly added to calculations and should be calculated separately.

17.1.1 RDT&E

In this part, cost of RDT&E phase will be estimated, estimated cost will be calculated by determining the cost of Engine, Avionics, payload and parachute system for aircraft's minor systems, and remaining cost elements for this phase will be calculated by using gathered data, Gundlach method and making some assumptions.

17.1.1.1 Engines and Avionics Cost

In this part, the cost of avionic and engines will be calculated to have an accurate cost estimation based on requirements and operation

17.1.1.1.1 Engine

Bottom-Up method is used to calculate propulsion system cost, this method ensures that this part doesn't make any error for further calculations. Off-the-shelf products considered for propulsion system to reduce the cost of engineering (compared to order or design a new product for propulsion system)

Table 17-1 Propulsion System component's cost

Name	Cost (USD)
3W-28i CS	750
Foam air filter	17.5
Propeller-CFK-3-blade 17/10	80
Muffler	128
Muffler holder	27
Teflon coupler	7

Exhaust manifold 3W-24i / 3W-28i	40
2-stroke Small Engine Fuel Injection Kit (from EcoTrons) [EFI report]	600
100W generator	200

From Table 17-1, Propulsion system's cost can be estimated and its cost will be 1850 USD.

17.1.1.1.2 Avionics

According to the same reasons that explained in propulsion system cost estimation, Bottom-Up method will be used in this part and off-the-shelf products and their cost will be considered.

Table 17-2 Avionics Components Cost

Name	Cost (USD)
Pixhawk 4 Autopilot and Neo-M8N GPS Combo	220
10 x Servo	3800
VN-100 IMU with Thermal Calibration	1300
Ping2020i (ADS-B transceiver + GPS + Baro)	2000
Heated Pitot-Static Probe	435
Marco Polo Locator	235

From Table 17-2 we can estimate Avionics cost for RDT&E Section. It should be mentioned that Ping2020i has a discount rate for ordering amount larger than 25 units, this discount will not be considered in RDT&E section, but will be used in manufacturing part. Estimated Cost for Avionics in this part will be 8000 USD.

17.1.1.2 Payload and Emergency Recovery System Cost

A set of payload and parachute will be purchased for Flight Tests and their cost should be calculated and considered in RDT&E cost estimation. Off-the-shelf products is used, and their costs are shown in Table 17-3.

Table 17-3 Payload Components Cost

Name	Cost (USD)
LT965R (EO camera)	3580
FLIR Vue 336 9mm	1500
OTUS-U200 Surveyor	42000

RIEGL miniVUX-1 UAV	50000

By using trends to estimate parachute system cost, cost of a parachute system will be assumed to be 900 USD per system.

For lack of data for Engineering and Tooling man-hour and Engineering and Tooling Cost, it is decided to use results of an article from MIT open access articles [resource], assumption of this article (that is used to design a UAV) is shown below:

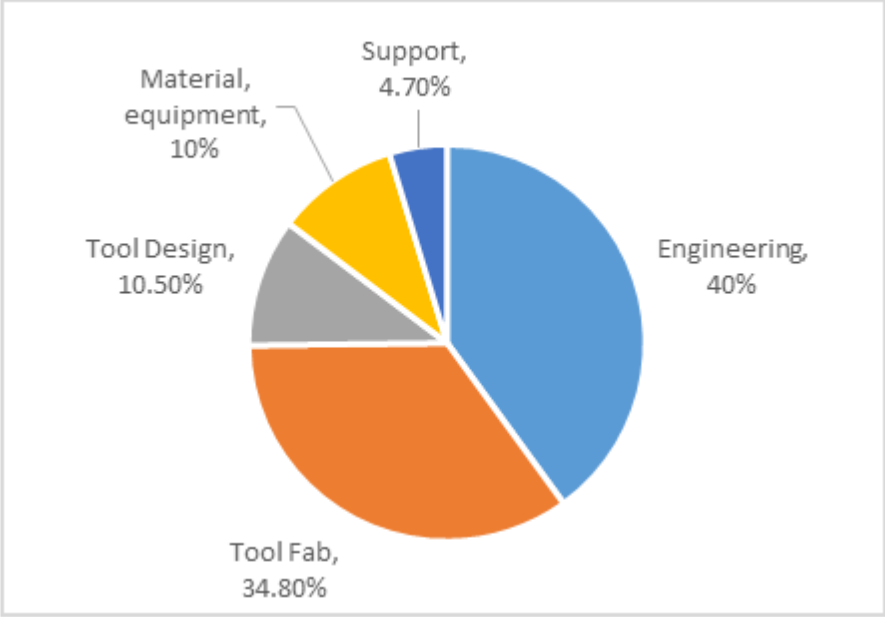

Figure 17–1 Cost breakdown by work category for a typical aircraft

By using Figure 17–1 as a reference and using gathered data for engineering man-hour estimation (source of this data wants to be anonymous), engineering and tooling cost for RDT&E phase can be determined.

To calculate manufacturing and materials cost Gundlach method [] has been used with this following assumptions:

- Number of Prototypes = 5
- RDT&E production rate = 1 unit/month
- Using composite for airframe

- Engineering dollar rate per hour = 120 USD
- Manufacturing labor rate per hour = 35 USD
- Tooling labor rate per hour = 60 USD
- Facilities Factor = 0.2
- Finance rate = 0.1

Mentioned calculations results in 1.767 million USD for total RDT&E cost, this total breaks down to:

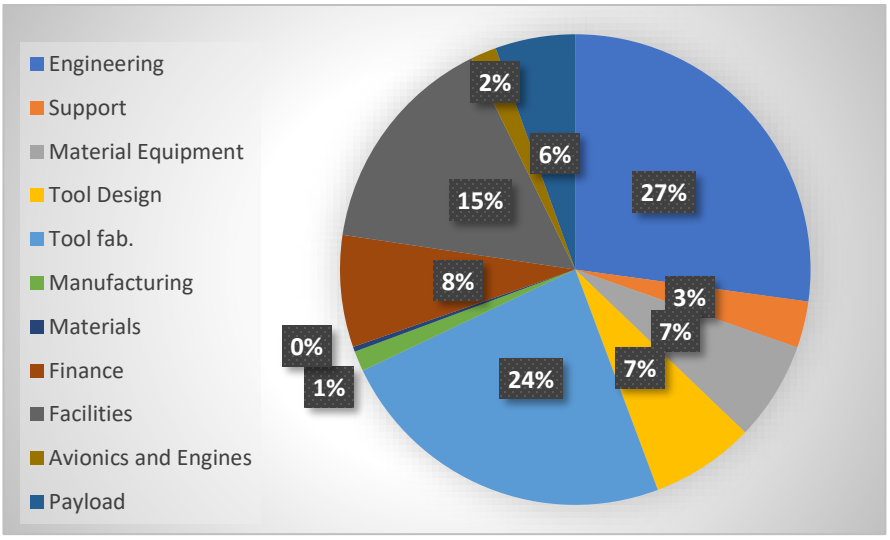

Figure 17–2 RDT&E Cost Breakdown

By calculating RDT&E cost, we can show the contribution of RDT&E cost and number of produced aircraft. This contribution has been shown in Figure 17–3.

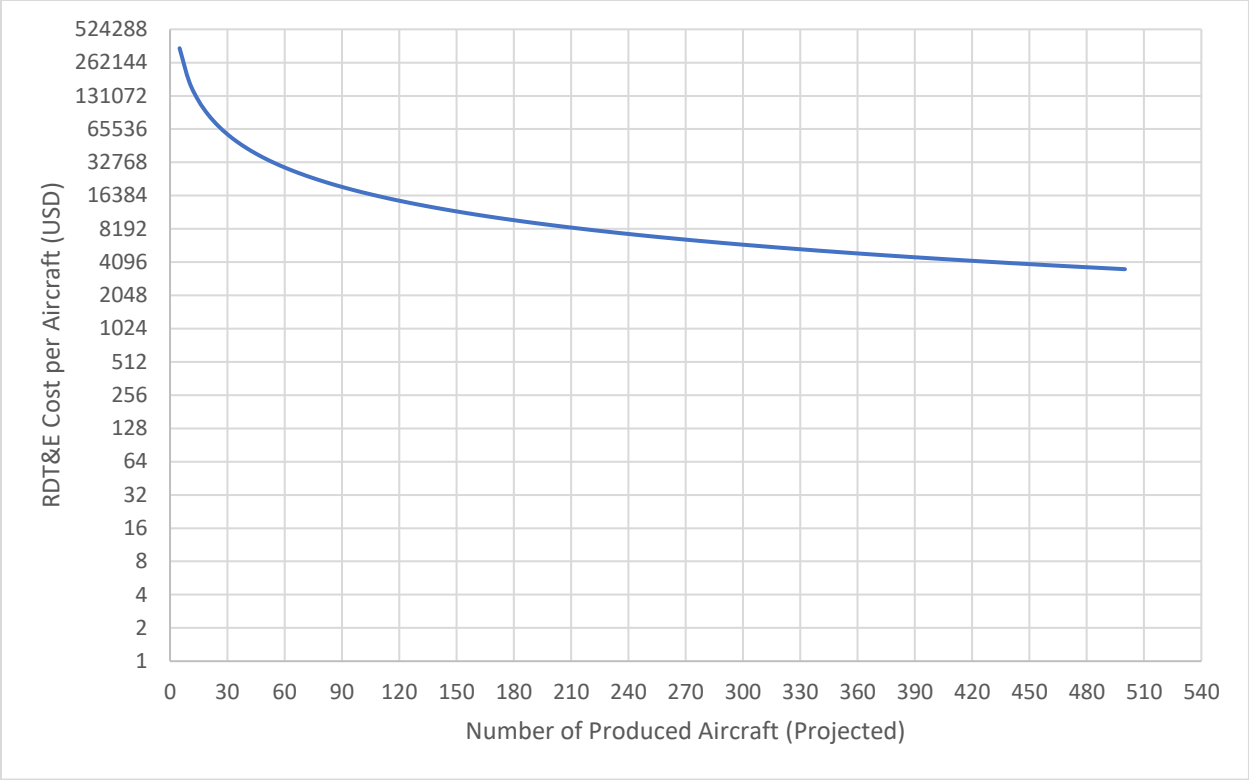

Figure 17–3 Contribution of RDT&E Phase with fly away Cost of aircraft

As you can see in Figure 17–3, it doesn't make sense to produce less than 180 (RDT&E cost per aircraft will be more than 10000 USD) units of aircraft and it makes financial sense to produce more than 290 units of aircraft. (RDT&E cost per aircraft will be less than 6000 USD)

17.1.2 Manufacturing

Description (method and purpose)

In lack of data for Engineering and Tooling Cost, Escalation of engineering and tooling cost in RDT&E and manufacturing phase has been considered, this escalation has been done by using Roskam method and will be applied in the results of RDT&E cost estimation section. It is needed to use some assumptions for calculating manufacturing cost:

- Manufacturing plan is based in production of 480 units of WAAPI
- Number of produced aircraft per month will be 16 units

- Engineering dollar rate per hour = 120 USD
- Manufacturing labor rate per hour = 35 USD
- Tooling labor rate per hour = 60 USD
- Overall profit for selling price will be at least 15%

Mentioned assumptions results is 11.424 million USD for total manufacturing cost, breakdown of this total is shown below:

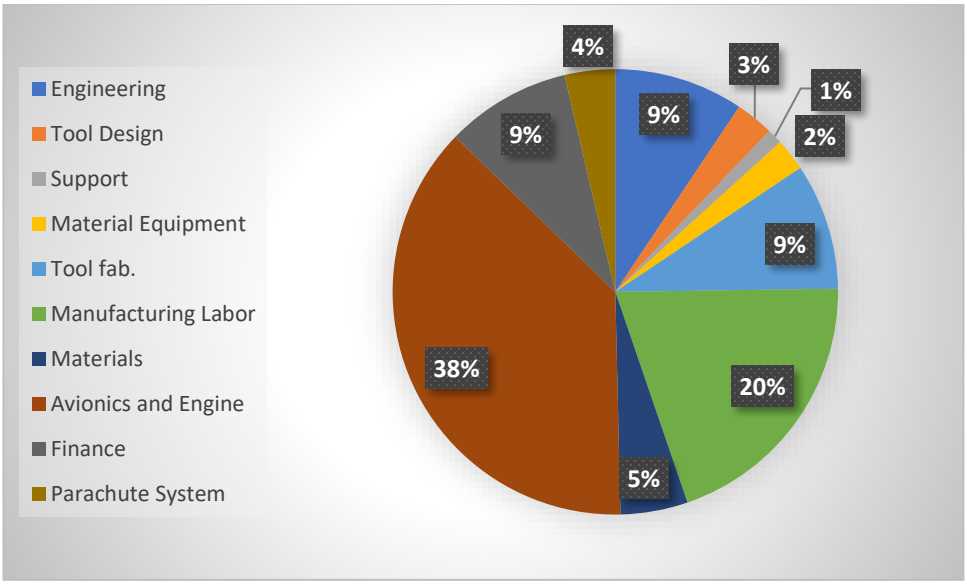

Figure 17–4 Manufacturing Cost Breakdown

By calculating RDT&E and manufacturing cost, flyaway and unit cost of UAV can be calculated.

Table 17-4 Flyaway and Unit Cost of WAAPI

Flyaway Cost (USD)	Profit Margin	Unit Cost (USD)
27500	15%	31200

Breakdown of flyaway cost can be found in Figure 17–5.

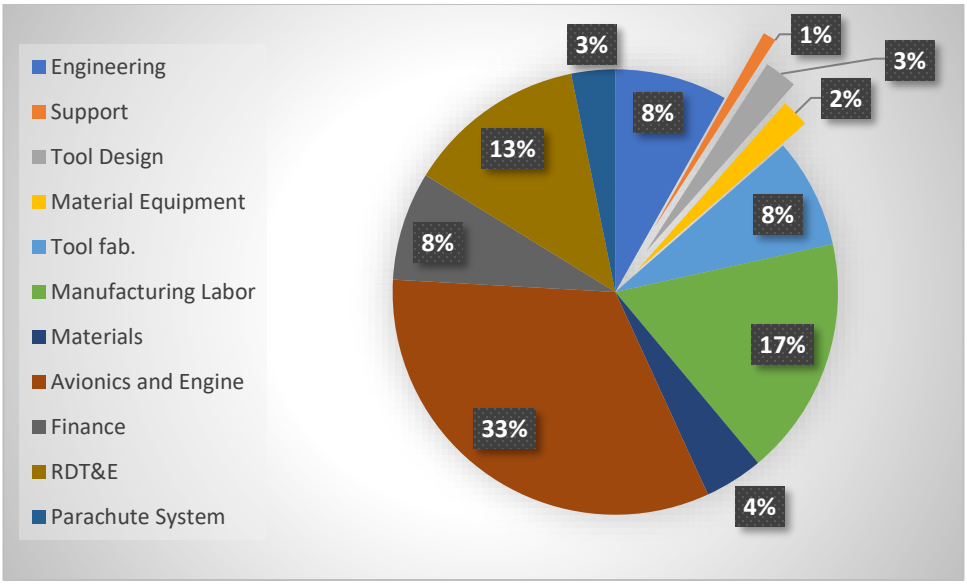

Figure 17–5 Flyaway Cost Breakdown

17.2 System Cost

In this part, cost of a full system will be estimated, components of the system will include ground control station, truck, shipping suitcase, aerial vehicle, car top launch mechanism, engine starter, and a set of payload. The truck is a 2018 Ford F-150 SuperCrew cab XL with 6.5 ft. box. Installation labor will be considered in the model (with the assumption of 4 man-hours needed to install car-top-launch mechanism and labor rate of 35 USD/hour) and in lack of data for car top launch mechanism, its cost will be estimated and will be assumed 2500 USD.

Cost of each system's element and installation labor has been estimated and can be found in Table 17-5.

Table 17-5 System element's cost

Element	Cost (USD)
Unmanned aerial vehicle	31200
Engine starter	90
2018 Ford F-150 SuperCrew cab	40010
EO/IR camera (incl. Gimbal)	47080
RIEGL miniVUX-1 UAV	50000
2x Shipping suitcase	1000
Car top launch mechanism	2500
Installation labor	140

Ground Control Station	6360
PingStation (all weather ADS-B receiver)	1750

From Table 17-5, it can be concluded that the whole system cost per unit will be 180150 USD. Breakdown of this cost is shown in Figure 17–6.

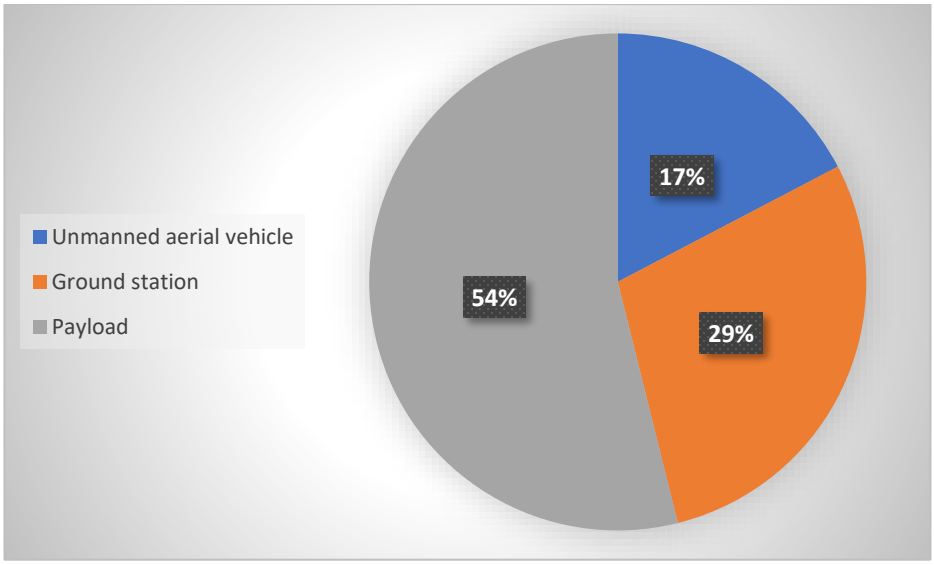

Figure 17–6 Breakdown of a system cost

17.3 Operating Cost

In this part, direct operating costs will be calculated by determining the fuel, maintenance, flight and cabin crew cost, engine replacement, and car battery replacement cost.

Gundlach [3] method will be use to estimate flight and cabin crew cost. Fuel cost will be calculated by using 200 mile mission (Figure 3–1) that last 3.5 hours. It is assumed that this mission will be performed 300 days per year and there is not enough time to perform this mission 2 times in a day.

17.3.1 Fuel Cost

To perform a mission with 200 miles of range, WAAPI requires 0.7 lb. of fuel (premium gas). Premium gas cost per gallon has an average of 2.34 USD/gallon, [8] and its cost for a single mission will be near 30 cents for every mission. This calculation results that the fuel cost of aircraft is not main concern.

17.3.2 Maintenance

According to “Designing Unmanned Aircraft Systems: A Comprehensive Approach” [3], assumption of 1 hour maintenance per operating days is a reasonable assumption (but maintenance will not occur every day) labor rate for a maintenance is will assumed 40 USD/hour [9] and maintenance cost for a single mission will be 40 USD.

17.3.3 Aircraft Engine Replacement

According to 3W’s operating manual for 3W-28i CS [10], guaranteed flight hours for 3W-28i CS is 1200 hours and with considering very expensive payloads for WAAPI (Table 17-5) risk of engine shut-down during flight is not reasonable and the aircraft’s propulsion system should be replaced after 1200 hours of operation. With considering Table 17-1 and typical mission, after 336 missions, propulsion system will be replaced with a new one and its cost for a single mission can be estimated 5.5 USD.

17.3.4 Truck Battery Replacement

Ground station will use truck battery to provide its energy and GCSD4 components normally using 5 Ah of energy for every mission. Typical battery capacity for Ford F-150 is 92 Ah and after 18 days work (or 18 typical mission), truck battery should be replaced and its replacement cost is near 200 USD and can be estimated 11 USD for a single mission.

17.3.5 Truck fuel cost

Based on trends, it is assumed that truck will pass near 90 miles to reach the operation area. Passing this distance will consume 4.7 US gallon. It is assumed that truck will use premium gas that also can be used in aircraft, so aircraft can use truck’s fuel to perform its mission. Cost of truck fuel cost for a single mission is near 22.16 USD and it will be considered in operating cost calculations.

17.3.6 Flight and cabin crew cost

By using “Designing Unmanned Aircraft Systems: A Comprehensive Approach” [3] estimation, labor hour rate for operator will assumed 90 USD/hour. Labor rate for cabin crew will be estimated by using Airport’s

ground crew labor rate and will be assume 45 USD/hour [11]. The same assumption in truck fuel cost part will be considered and a reference timeline will be assumed to calculate flight and cabin crew cost. This reference timeline is shown in Table 17-6.

Table 17-6 Reference Timeline for operating cost calculations

Reach the operation area	Setting up the UAS	Operation	Packing the UAS	Leave the operating area and come back to station
2 hours	15 minutes	3.5 hours	15 minutes	2 hours

By using Table 17-6 as a reference, Flight and cabin crew cost for a single mission will be 1080 USD.

After calculating cost of direct operating cost elements, direct operating cost per flight hour can be estimated. This estimation results 324 USD per flight hour. Breakdown of direct operating cost is shown in Figure 17–7.

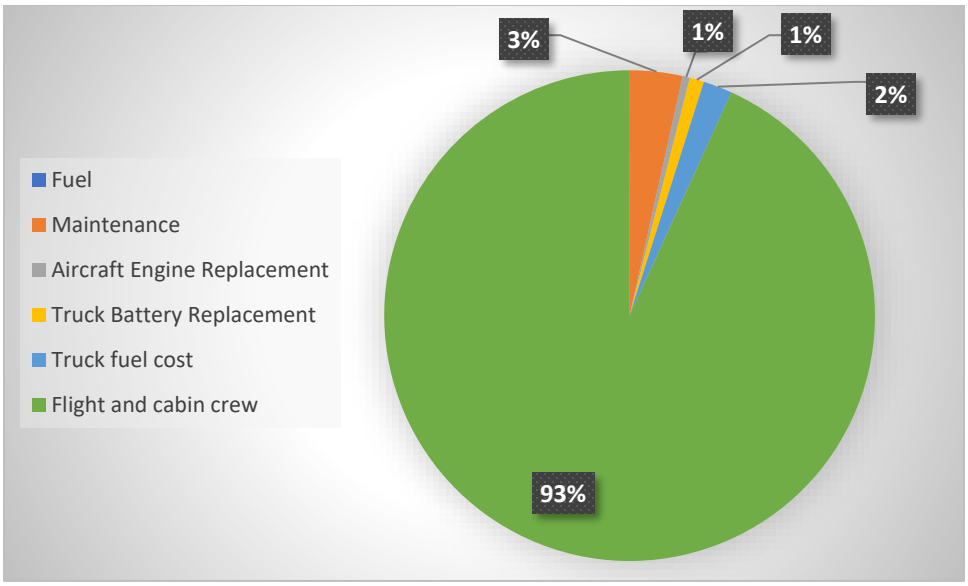

Figure 17–7 Direct operating cost breakdown for system

As it shown in Figure 17–7, 93% of the direct operating cost (for a complete system) is for flight and cabin crew and aircraft has an unimportant rule in direct operating cost (near 12.8 USD).

18 References

[1] Mordor Intelligence, Mordor Intelligence, [Online]. Available: https://www.mordorintelligence.com.

[2] J. Roskam, Airplane Design, 1985.

[3] D. P. RAYMER, Aircraft design: a conceptual approach, 1989.

[4] J. Gundlach, Designing Unmanned Aircraft Systems: A Comprehensive Approach, 2012.

[5] M. H. Sadraey, Aircraft Design A System Engineering Approach.

[6] M. C.-Y. N. Chunyun Niu, Airframe Structural Design.

[7] N. a. W. R. Prasad, Aerospace Materials and Material Technologies.

[8] K. Abdurohman, F. Ari Wandono and D. Hidayat, Design and Stress Analysis of LSU 05 Twin Boom Using Finite Element Method.

[9] 3w-modellmotoren, [Online]. Available: https://3w-modellmotoren.de/wp-content/uploads/2016/11/Operating-Manual.pdf.

[10] EcoTrones, [Online]. Available: https://www.ecotrons.com/small_engine_fuel_injection_kit/2_stroke_small_engine_fuel_injection_kit/.

[11] Skygraphics, [Online]. Available: http://uavpropulsiontech.com/skygraphics/.

[12] A. Hobbs and S. R. Herwitz, Human Factors in the Maintenance of Unmanned Aircraft.

[13] K. Mays. [Online]. Available: https://www.cars.com/articles/why-is-premium-gas-so-expensive-1420683350396/.

[14] Payscale, [Online]. Available: https://www.payscale.com/research/US/Job=Aircraft_Maintenance_Technician/Hourly_Rate.

[15] Salary.com, [Online]. Available: https://www1.salary.com/flight-attendant-hourly-wages.html.

[16] K. Hieu Ngo and H. Thien Loc, Airfoil Selection for Fixed Wing of Small Unmanned Aerial Vehicles, 2016.

[17] I. Nikolov and C. Madsen, LiDAR-based 2D Localization and Mapping System using Elliptical Distance Correction Models for UAV Wind Turbine Blade Inspection, 2017.

[18] M. C. Butler and R. Montanez, How to Select and Qualify a Parachute Recovery System for your UAV.

[19] RIEGL Laser Measurement Systems, [Online]. Available: http://www.riegl.com.